Foundations of DC plasma sources

View the article online for updates and enhancements.

Related content

- Foundations of low-temperature plasma physics—an introduction
  A von Keudell and V Schulz-von der Gathen

- Low-pressure gas discharge modelling
  G G Lister

- Glow discharges with electrostatic confinement of fast electrons
  V I Kolobov and A S Metel

Recent citations

- Electrical breakdown from macro to micro/nano scales: a tutorial and a review of the state of the art
  Yangyang Fu *et al*

- A modern perspective on flow instability and shockwave phenomena in reacting gas multiphase system excited by direct current
  Peter F. Kurbatov

- On the Similarities of Low-Temperature Plasma Discharges
  Yangyang Fu and John P. Verboncoeur
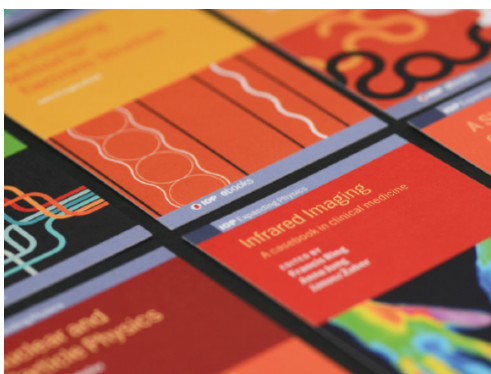
IOP ebooks™

Bringing together innovative digital publishing with leading authors from the global scientific community.

Start exploring the collection–download the first chapter of every title for free.

Topical Review

Foundations of DC plasma sources

Jon Tomas Gudmundsson[1,2] and Ante Hecimovic[3,4]

[1] Science Institute, University of Iceland, Dunhaga 3, IS-107 Reykjavik, Iceland
[2] Department of Space and Plasma Physics, School of Electrical Engineering, KTH–Royal Institute of Technology, SE-100 44, Stockholm, Sweden
[3] Institute for Experimental Physics II, Ruhr-University Bochum, D-44801 Bochum, Germany
[4] Max-Planck-Institut for Plasma Physics, Boltzmannstraße 2, D-85748 Garching, Germany

E-mail: tumi@hi.is

Abstract
A typical dc discharge is configured with the negative cathode at one end and a positive anode at the other end, separated by a gas filled gap, placed inside a long glass cylinder. A few hundred volts between the cathode and anode is required to maintain the discharge. The type of discharge that is formed between the two electrodes depends upon the pressure of the working gas, the nature of the working gas, the applied voltage and the geometry of the discharge. We discuss the current–voltage characteristics of the discharge as well as the distinct structure that develops in the glow discharge region. The dc glow discharge appears in the discharge current range from μA to mA at 0.5–300 Pa pressure. We discuss the various phenomena observed in the dc glow discharge, including the cathode region, the positive column, and striations. The dc glow discharge is maintained by the emission of secondary electrons from the cathode target due to the bombardment of ions. For decades, the dc glow discharge has been used as a sputter source. Then it is often operated as an obstructed abnormal glow discharge and the required applied voltage is in the range 2–5 kV. Typically, the cathode target (the material to be deposited) is connected to a negative voltage supply (dc or rf) and the substrate holder faces the target. The relatively high operating pressure, in the range from 2 to 4 Pa, high applied voltages, and the necessity to have a conductive target limit the application of dc glow discharge as a sputter source. In order to lower the discharge voltage and expand the operation pressure range, the lifetime of the electrons in target vicinity is increased through applying magnetic field, by adding permanent magnets behind the cathode target. This arrangement is coined the magnetron sputtering discharge. The various configurations of the magnetron sputtering discharge and its applications are described. Furthermore, the use of dc discharges for chemical analysis, the Penning discharge and the hollow cathode discharges and some of its applications are briefly discussed.

Keywords: dc glow discharge, low-temperature plasmas, gas discharge, dc sputter source

1. Introduction

The dc discharge is a basic and a very easily reproducible source of plasma. It is typically configured with the negative cathode at one end and a positive anode at the other end separated by a gas filled gap, sitting inside a long glass cylinder. The plasma is created by applying a dc voltage over the gas filled gap between two electrodes. Such dc discharge

has been the subject of intensive research for almost 200 years. The dc discharge and in particular the dc glow discharge is important historically, both for studying the properties of the plasma as well as for the various applications where the dc discharge is used to provide a weakly ionized plasma.

The term gas discharge refers to the flow of electric current through a gaseous medium. If this is to occur, some of

the gas atoms and molecules have to be ionized. Furthermore, there has to be an electric field to drive this current. The current, which provides power to the discharge, has to be continuous throughout the length of the discharge. In the dc discharge, the current is driven by both ions and electrons created within the plasma volume, as well as by electrons emitted from the cathode. Therefore, for a comprehensive description of the dc discharge current, the interaction of charged particles with the electrode surfaces has to be taken into account.

The electrons and ions are charged so that application of electric or magnetic field can preferentially heat these particles while the neutral particles remain at lower temperature. A species temperature is a measure of the average energy of that species energy distribution. The various types of particles are generally not in thermal equilibrium, which means that the temperature of the different plasma species is not the same. In particular, the electrons, due to their low mass, can be easily accelerated to high energies sufficient to excite and ionize neutral atoms or molecules. Thus, the electrons have much higher temperature than the heavy particles (ions, atoms, and molecules), or $T_e \gg T_i, T_g$, where T_e is the electron temperature, T_i is the ion temperature, and T_g is the neutral gas temperature.

The gas pressure is an important parameter influencing the plasma species temperature and thermal equilibrium between species. At low pressure only a few collisions occur and the energy transfer between species is inefficient. At high pressure many collisions occur between the various plasma species which results in more equal temperatures of the species. The mean free path is the average distance traveled by a particle between collisions with other particles and is reciprocal to the product of gas pressure and the collisional cross section.

The focus of this work is on presenting the fundamental properties of the dc discharge and some of its applications. The dc discharge has numerous diverse applications, such as being a source of illumination, as gas lasers, an electron source for Hall thrusters, a pixel in a plasma display panel (PDP), and as a sputter deposition tool. Section 2 gives a general description of the dc discharge, through the development of the voltage–current relationship as the current increases. The axial profile of the various parameters of the dc glow discharge is discussed in section 3. We discuss the electrical breakdown condition and the Paschen curve in section 4.1, the secondary electron emission from the cathode that plays a significant role in maintaining the discharge, in section 4.2, and the cathode sheath in section 4.3. The sputter process and the application of the dc discharge as a sputter source, or the diode sputter source, are discussed in section 5. We discuss how and why the dc sputter source was developed into the magnetron sputtering discharge in section 6, where also the various configurations of magnetron sputtering discharges are presented. We finally briefly discuss the application of dc discharge to chemical analysis of surfaces in section 7, the Penning discharge in section 8 and the hollow cathode discharge in section 9.

2. The dc discharge

Let us assume two parallel electrodes with applied potential V_D separated by distance L, placed in a glass vessel. The gap between the electrodes is filled with gas at pressure p. The type of discharge formed between the two electrodes depends upon the (i) pressure of the working gas, (ii) the nature of the working gas, (iii) the applied voltage, and (iv) the geometry of the discharge. A discussion of the relationship between the discharge current and the applied voltage for the dc discharge can be found in review articles such as by Druyvesteyn and Penning (1940), Francis (1956) and Ingold (1978) and in a number of textbooks including those by Howatson (1976, chapter 4), Raizer (1991, section 8.2), and Roth (1995, chapter 9). The early history of discharge physics research is given in a brief review by Brown (1978), where some of the terminology used in discharge physics is explained, and some of the historical people, whose names are associated with the various phenomena observed in the dc discharges, are introduced. A typical representation of the relationship between the discharge voltage and the discharge current across a low pressure dc discharge is shown in figure 1. The discharge is connected in series with a variable resistance R, that controls the current flowing through the circuit as shown by the circuit diagram in figure 2. The discharge voltage is

$$V_D = V_S - I_D R, \quad (1)$$

where V_S is the voltage at the output of the voltage source and I_D is the discharge current. The curve shown in figure 1 can be traced out by varying the load resistance R and/or the output voltage of the source V_S. When a voltage is first applied, the current is very low. This current consists of contributions from various random sources such as cosmic radiation. Initially this current remains nearly constant with increased voltage. As the voltage is increased further (either by increasing V_S or lowering R), the charged particles eventually achieve enough energy to produce more charged particles though collisions with the gas atoms or bombardment of the electrodes (e.g. secondary electrons). As more charged particles are created the current increases, while the voltage is limited by the output impedance of the power supply and remains roughly constant. This region is commonly referred to as the *Townsend discharge*. The characteristics of the Townsend discharge are the very small currents and uniform electric field distribution across the entire discharge. Space charges have little influence and a sheath has not developed in the cathode vicinity. The Townsend discharge is not luminous since the electron density is low and therefore the density of excited atoms, which emit visible light, is correspondingly small. Furthermore, it is not a self-sustained discharge in the sense that it does not entirely provide its own ionization but requires some external assistance in order to produce electrons either in the gas itself or from a negative electrode. Since the current is small and the electron density is very low, the Debye length is large and comparable to the system characteristic length L, such that the electric field penetrates into the discharge.
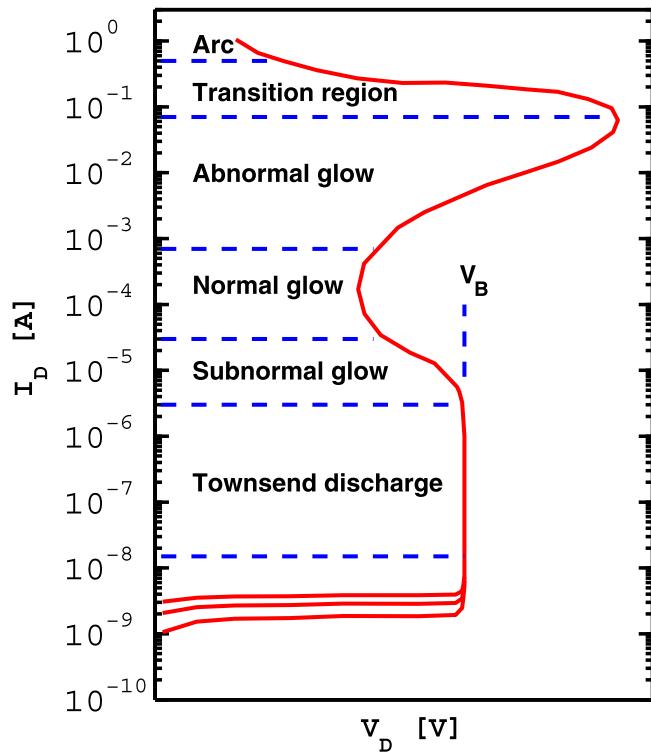
Figure 1. The discharge current versus applied voltage for a dc discharge.

Figure 2. A circuit diagram showing the voltage source, the variable resistor that controls the current flow through the circuit, and the dc discharge.

If the voltage is increased further, the current increases and eventually this leads to an ionization avalanche, which results in the current sharply increasing by several orders of magnitude. As the current increases, an accumulation of electrons and ions occurs in front of the electrodes that deforms the field structure. By increasing the current, thus increasing the electron density, space charge distortion sets in, and the Debye length decreases and eventually a sheath, with high field strength, is formed next to the cathode. This is what is referred to as the breakdown point, and transition to the *subnormal glow*. It occurs at voltages ranging from two to three hundred volts upwards, depending on the nature of the gas, pressure, and the separation of the electrodes. Once a breakdown has occurred, the discharge becomes self-sustaining, the gas becomes luminous, and takes the form of a glow. The ions from the plasma are accelerated towards the negative electrode, i.e. cathode, bombarding it at energies comparable to the value of the applied voltage. As the ions bombard the electrode, secondary electrons are emitted, accelerating away from the negative cathode, gaining sufficient energy to excite and ionize the atoms of the working gas. Thus, in turn, more ions are available to bombard the cathode, and create more secondary electrons.

When the number of electrons generated is high enough to generate enough ions, to produce the equal number of electrons, the discharge is said to be self-sustaining. At this condition the voltage across the discharge drops and the current increases abruptly. The voltage drop indicates a more

efficient ionization processes and/or reduced loss. The current is now dictated not only by the output resistance of the power supply but the discharge resistance as well. This is referred to as the *normal glow* or the dc glow discharge. The electron impact excitation of atoms and ions by collisions, followed by de-excitations through emission of the radiation is responsible for the characteristic glow of the normal glow. The ion bombardment is initially not uniformly distributed across the cathode surface. The discharge current arranges an optimum current density and if the current increases further, more and more of the cathode surface participates. This will continue as the supplied power is increased until a nearly uniform density is achieved covering the whole cathode area and the plasma becomes homogeneous.

In case the power is reduced at this point beyond a critical value, the transition from a homogeneous plasma to a structured plasma is observed for a dc micro-discharges in xenon, with distinct patterns emerging in the formerly homogeneous plasma layer (Schoenbach *et al* 2004). The plasma pattern consist of filamentary structures arranged in concentric circles. With further reduction in current the number of filaments decreases to a minimum before the discharge extinguishes. The number of filaments and the degree of rotational symmetry depend on the gas pressure.

When the entire available cathode surface is covered by ion bombardment, a further increase in the applied power leads to an increase in both voltage and current. This region is referred to as the *abnormal glow* and is the regime used for sputtering and is discussed in section 5. The abnormal glow discharge looks much like the normal glow discharge but is more intensely luminous, and sometimes the structures near the cathode (discussed in section 3) merge into one another. When increasing the current density further from the abnormal glow state, the discharge transfers into arc. The kinetic energy of ions bombarding the cathode is transferred to the vibration excitation of the cathode atoms, thus heating the cathode surface. When the cathode surface gets hot enough, the electrons are emitted via thermionic emission and the discharge makes a transition into the *arc* regime, a plasma state characterized by low voltage and high-current.
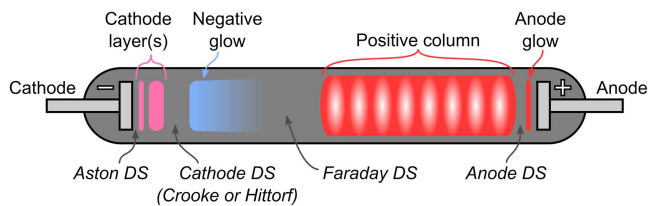
Figure 3. A schematic of the dc glow discharge showing the several distinct regions that appear between the cathode and the anode.

Figure 4. The structure of a nitrogen dc glow discharge with a stratified positive column. The cathode is on the left and the anode on the right. Reproduced from Lisovskiy *et al* (2012). © IOP Publishing Ltd. All rights reserved.

To summarize the above discussion: dc discharges in steady state can be classified in three types according to the current which they carry. These are:

- The Townsend discharge for discharge currents up to 10^{-6} A.
- The glow discharge for discharge currents in the range 10^{-6}–10^{-1} A.
- The arc discharge for discharge currents higher than 10^{-1} A.

3. The dc glow discharge

Over time, the simplicity of the dc glow discharge geometry made it a commonly used plasma generation method for fundamental research in both discharge physics and atomic and molecular physics. The low pressure dc glow discharge has a very distinctive appearance which is shown schematically in figure 3. Here, we will discuss these structures and the role of each region. This topic has been under investigation for almost 200 years so the literature is rather extensive. Such a discussion can be found in a number of review articles (Druyvesteyn and Penning 1940, Francis 1956, Ingold 1978) and textbooks such as Roth (1995, chapter 9) and Raizer (1991, section 8.1).

As seen in figure 1, the dc glow discharge operates the discharge current range from μA to hundreds of mA (*current density* in the range 10^{-7}–10^{-2} A cm^{-2}). Furthermore, the pressure is typically in the range 0.5–300 Pa. The plasma that is formed in a low pressure dc glow discharge can exhibit a structure of several distinct regions, bands of varying luminosity and color, between the cathode and the anode as seen in the schematic in figure 3. These structures appear over a wide range of operating conditions. A photograph of the dc glow discharge showing some of the structure is shown in figure 4.

The cathode is often made of an electrically conductive metal. The discharge is maintained by electrons emitted from the cathode as a result of positive ion bombardment of the cathode surface, referred to as secondary electron emission and discussed in section 4.2. The potential difference applied between the two electrodes is generally not equally distributed between cathode and anode. Immediately next to the cathode is the *primary dark space* or the *Aston dark space* where the secondary electrons are accumulated. This region has a strong electric field and a negative space charge, do to
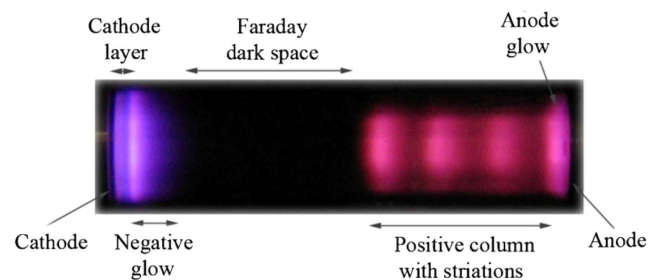
the accumulation of slow electrons which are in the process of being accelerated from the cathode.

Next to the Aston dark space is the *cathode glow* (a bright reddish or orange fluorescence at the cathode surface seen in figure 4) with a relatively high ion density. Here, the secondary electrons begin to accelerate away from the cathode to a very high velocity. These high energy electrons start to have collisions with neutral gas atoms at a distance away from the cathode corresponding to the mean-free-path, the cathode glow. The color of the light emitted is characteristic of both the cathode material and the working gas. The axial length of the cathode glow depends on the nature of the gas and gas pressure.

The cathode glow is followed by the *cathode (Crookes or Hittorf) dark space* where the electric field is moderate and the space charge is positive and of relatively high density. In this dark space, the positive ions are also accelerated towards the cathode. Since the mobility of ions is much less than that of electrons, this dark space consists mainly of ions. The cathode dark space is followed by the *negative glow*. The negative glow exhibits the brightest light intensity of the entire discharge (see figure 4). The acceleration of the secondary electrons leads to excitation and ionizing collisions in this region. Here, the electric field is relatively low and the current is almost entirely carried by electrons.

Figure 5 shows the spatial variations of the potential, the electric field, particle densities, space charge and current densities along the axis of a dc glow discharge. The spatial variation of the plasma parameters shown here was found by particle-in-cell simulation of an argon discharge at 50 Pa when a voltage of 400 V is applied across the 5 cm discharge gap (the cathode is kept at −400 V) (Budtz-Jørgensen 2001). As the potential profile indicates (figure 5(a)), the electric field is large in the vicinity of the electrodes and almost zero in the plasma bulk. Thus, almost all the potential drops in the first few millimeters in front of the cathode. We see in figure 5(c) that the sheath region is depleted of electrons and, in figure 5(d), we see that the net space charge is positive in the sheath region. The space charge shown in figure 5(d) is found by subtraction of the electron density from the ion density. In

a)

b)

c)

d)

e)
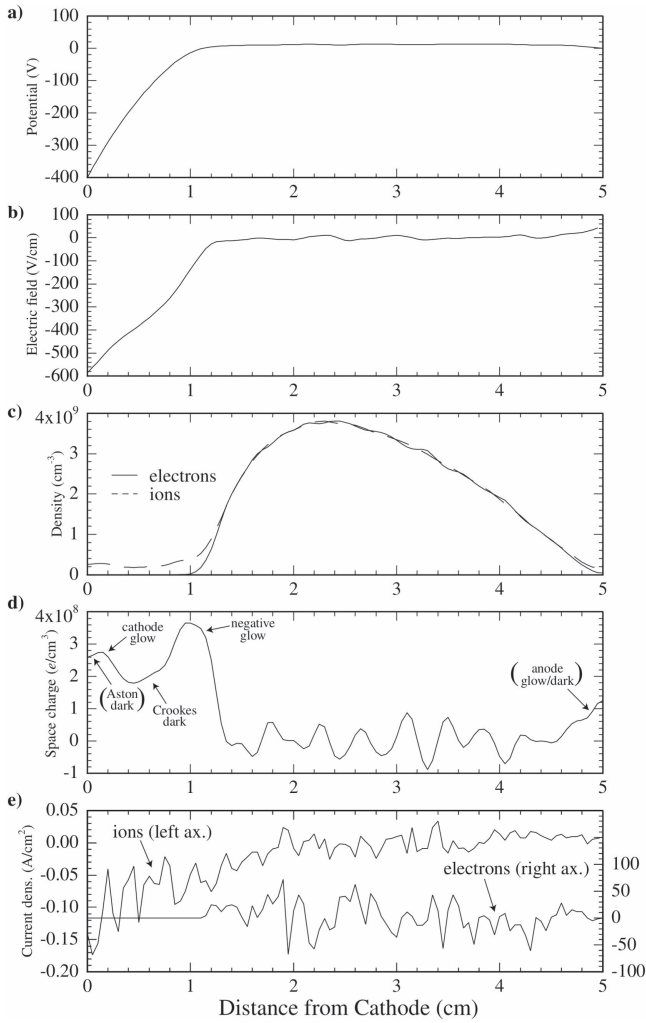
Figure 5. Spatial profiles of (a) the plasma potential, (b) the electric field, (c) ion and electron density, (d) space-charge density, and (e) ion and electron current density. From particle-in-cell simulation of an argon discharge at 50 Pa and −400 V applied to the cathode. Reproduced with permission from Budtz-Jørgensen (2001).

the plasma bulk, the plasma is quasi-neutral and the electron and ion densities are the same. This space charge density leads to the electric field distribution seen in figure 5(b). We see from the above discussion that most of the voltage drop across the discharge appears over the cathode sheath. The cathode sheath size, the distance from the cathode surface to the boundary of the negative glow is denoted by d_c. The voltage drop is referred to as the cathode fall of V_c volts. Furthermore, most of the power dissipation in the glow discharge occurs in the cathode region. The electric field within the cathode sheath has been experimentally determined (Doughty *et al* 1987, Den Hartog *et al* 1988) using optogalvanic diagnostics (Doughty *et al* 1985). The measurements show that the electric field exhibits a linear decrease in the cathode sheath with a gradient that depends on the current density, showing that in principle the sheath thickness is independent of the current density for a helium discharge

at 466 Pa (Doughty *et al* 1987, Den Hartog *et al* 1988). Similarly, Booth *et al* (1994) applied a laser-induced fluoresence to measure a roughly linear decrease in the electric field strength as a function of distance from the cathode in hydrogen discharge. They see decreasing sheath thickness with increasing neutral gas pressure.

The negative glow is followed by the *Faraday dark space* where the electric field is low as well as the energy of electrons. The electrons do not have enough energy to excite the atoms or molecules of the working gas and electrons recombine with ions. Thus this appears as a dark region in figure 4. The Faraday dark space is followed by *the positive column*. The positive column is a quasi-neutral plasma where the electric field is very low. The positive column appears as a long uniform glow, except when striations are formed (in figure 4 striations appear in the positive column). The positive column is a quasi-neutral plasma that acts as a conducting path between negative glow region and the anode and will be discussed further below (section 3.1). Often a thin dark space is observed at the end of the positive column and a glow at the anode surface. *The anode dark space* has a negative space charge due to electrons that flow from the positive column to the anode. Close to the anode, electrons are attracted and accelerated, but ions are repelled. The accelerated electrons excite atoms or molecules, so the *anode glow* is a bright region that appears at the anode (see figure 4). The drift velocity of the electrons in the positive column is low as the electric field is weak and typically less than the electrons thermal velocity. This calls for a retarding electric field in front of the anode to prevent the full thermal electron current from reaching the anode. Recall that the anode must be positive with respect to the positive column in order to maintain the current. This leads to formation of a double layer. But the voltage drop in this region is small and plays little role in the overall discharge dynamics.

The size, intensity and color of all the regions described above are dependent on the working gas, gas pressure, and applied voltage. Also, some of the features may be absent over particular parameter ranges. The various gases exhibit a discharge of a characteristic color. The colors of the light emitted from the various zones of the dc glow discharge are listed in table 1. If the pressure is reduced, the cathode dark space expands at the expense of the positive column. This is due the fact that now the electrons have to travel farther (the mean free path is longer) to produce efficient ionization. For a secondary electron emission yield in the range 0.05–0.1 each secondary electron must produce roughly 10–20 ions to maintain the glow discharge. The discharge current at the cathode consists of electron current I_e and ion current I_i, or

$$I_D = I_e + I_i = I_i(1 + \gamma_{see}), \tag{2}$$

where γ_{see} is the secondary electron emission yield, so at the target, the dominating fraction of the discharge current is due to ions. Thus, at the cathode, most of the current is

Table 1. The color of selected luminous zones in the dc glow discharge. Based on Francis (1956).

Gas	Cathode layers	Negative glow	Positive column
He	red	pink	red/pink
Ne	yellow	orange	red/brown
Ar	pink	dark blue	dark red
H_2	red/brown	pale blue	pink
O_2	red	yellowish/white	pale yellow/pink center
N_2	pink	blue	red/yellow
Air	pink	blue	red/yellow

carried by ions flowing towards the cathode while in other regions of the discharge including the negative glow and the Faraday dark space nearly all the current is carried by electrons. This shows that the ionization processes in the cathode dark space are essential for the maintenance of the discharge. Den Hartog *et al* (1988) determined experimentally the ratio of ion to electron current at the cathode, to be 3.3 for helium discharge at 466 Pa showing almost no dependence on the total discharge current. Furthermore, they found that the majority of ions hitting the cathode are produced within the cathode sheath, and that the discharge current is almost solely carried by beam electrons at the boundary between the cathode sheath and the negative glow. How many ions each secondary electron produces depends on its mean free path and the distance between the anode and cathode. This relation is qualitatively the statement of Paschen's law that relates the breakdown voltage V_B to the product of gas pressure and electrode separation and will be discussed in section 4.1.

3.1. The positive column

If the length of the discharge tube is multiple times the radius of the tube, then most of the tube is filled with what appears to be a glow of uniform light intensity. This is the positive column. The positive column constitutes a quasi neutral plasma. Its sole role is to maintain conduction of current by electrons, which is established in the cathode vicinity. When a typical dc glow discharge is operated at a fixed pressure and the length is reduced, the length reduction is taken up entirely by the positive column, and the other regimes remain unchanged. This continues until the anode has reached the negative glow, at which point the voltage required to maintain the discharge begins to rise.

The positive column is a weakly ionized plasma often with cylindrical geometry, bounded by non-conducting walls and sustained by an axial current. The positive column is axially uniform and azimuthally symmetric and the various parameters vary only radially. Its properties are independent of the length of the column and it can be exptended infinetely. As the charged particles are lost to the tube walls the discharge is not radially uniform. The positive column is luminous as the electrons have energy high enough to ionize atoms and thus to excite atoms. The color of the positive column is characteristic of the gas and is generally not the same as that of the negative glow, nor is it as luminous. The electron or ion density is typically in the range 10^{15}–10^{16} m^{-3} within the positive column. The potential decreases radially and thus confines the electrons while driving the ions outwards towards the walls. At steady state there is a balance between the electron–ion pairs created via electron impact ionization in the bulk and the electron–ion pairs lost to the walls. Within the positive column, the only ionization that takes place is to compensate for losses do to recombination and diffusion to the chamber walls. The relative importance of these processes depends on the geometry of the discharge, gas pressure, and the current flow.

Most of the theoretical treatments of the positive column have been based on the classical ambipolar theory of Schottky (1924) and the free fall theory of Tonks and Langmuir (1929). This is how the positive column is often described in review articles (Ingold 1978), and in text books for pedagogical purposes including Roth (1995, section 9.2), Cherrington (1979, chapter 8), and Lieberman and Lichtenberg (2005, section 14.2). In this treatment, referred to as the local approach, the electron energy distribution is often assumed to be Maxwellian, the Boltzmann equation is not solved, and that one-step ionization of the working gas is the sole electron source. The electrons are assumed to be in equilibrium with the axial electric field and the average electron energy is radially invariant in this assumption. Within the positive column the quantities such as the electric field and electron and ion densities are assumed to be independent of the longitudinal position and depend only on the radial distance from the tube walls. Hence, there is a balance between the production of charged particles by ionizing collisions of energetic electrons with neutrals and loss of charged particles by diffusion towards the tube walls where they recombine. This can be written as a particle balance

$$-\nabla \cdot D_a \nabla n = \nu_{iz} n, \tag{3}$$

where $n = n_e = n_i$ is the plasma density, D_a is the ambipolar diffusion coefficient, $\nu_{iz} = k_{iz} n_g$ is the electron impact ionization rate, and k_{iz} is the electron impact ionization rate coefficient. The electron impact ionization rate coefficient can be written

$$k_{iz} = \sigma_0 \bar{v}_e \left(1 + \frac{2T_e}{\mathcal{E}_{iz}}\right) \exp\left(-\frac{\mathcal{E}_{iz}}{T_e}\right), \tag{4}$$

where $\sigma_0 = \pi (e/4\pi\epsilon_0 \mathcal{E}_{iz})^2$, $\mathcal{E}_{iz}$ is the ionization potential, and we have assumed a Thomson cross section that is expanded near $\mathcal{E} = \mathcal{E}_{iz}$, and $\bar{v}_e = (8eT_e/\pi m)^{1/2}$ is the mean speed of electrons with a Maxwellian velocity distribution at temperature T_e (Lieberman and Lichtenberg 2005, p 71 and 79). Thus we can use the term electron temperature to describe the average energy of the electron gas. Here, we

use the roman typeface symbol T for the voltage equivalent of the temperature.

When the flux of electrons and ions to an insulating wall is equal the plasma has achieved a steady state. As the electrons are significantly lighter than ions, they have much higher mobility, so that an electric field is created to maintain a local flux balance. The diffusion coefficient that describes the ion and electron diffusion to the tube walls in steady state, is referred to as the ambipolar diffusion coefficient (see Lieberman and Lichtenberg (2005, pp 135–6) or Roth (1995, pp 157–8). When the mobilty of electrons is much larger than the mobilty of ions, we find that $D_a \approx D_i(1 + T_e/T_i)$ where $D_i = eT_i/M_i \nu_{mi}$ is the ion diffusion coefficient, M_i is the ion mass, $\nu_{mi} = n_g k_{mi}$ is the ion momentum transfer frequency, and k_{mi} is the ion momentum transfer rate coefficient. In general k_{mi} depends on the gas temperature T_g and the ion temperature T_i. For $T_e \gg T_i$ we see that $D_a \approx eT_e/M_i \nu_{mi}$ and the ambipolar diffusion coefficient is much greater than the diffusion coefficient for the ions. Following Schottky (1924) and Cobine (1958, section 8.11), the ion particle balance equation can be written in cylindrical coordinates

$$\frac{d^2n}{dr^2} + \frac{1}{r}\frac{dn}{dr} + \frac{\nu_{iz}}{D_a}n = 0 \tag{5}$$

which is Bessel's equation. The solution of Bessel's equation is

$$n(r) = n_0 J_0\left(r\sqrt{\frac{\nu_{iz}}{D_a}}\right), \tag{6}$$

where J_0 is a Bessel function of zero order and n_0 is the plasma density on the discharge axis, which will be determined later in terms of the discharge current. If the ion–neutral mean free path and the sheath thickness are both small compared to the column (tube) radius, or $\lambda_i, s \ll R$, then $n(R) \approx 0$ and we have

$$\sqrt{\frac{\nu_{iz}}{D_a}} = \frac{\chi_{01}}{R}, \tag{7}$$

where $\chi_{01} \approx 2.405$ is the first zero of the Bessel function of zero order. Both the ionization rate ν_{iz} and the ambipolar diffusion coefficient D_a depend on the electron temperature. If equation (4) is substituted into equation (7), we find that

$$\frac{\sigma_0 \bar{v}_e\left(1 + \frac{2T_e}{\mathcal{E}_{iz}}\right)}{eT_e/M_i k_{mi}}\exp\left(-\frac{\mathcal{E}_{iz}}{T_e}\right) = \left(\frac{\chi_{01}}{Rn_g}\right)^2 \tag{8}$$

which can be solved for T_e. This can be approximated, given $T_e \ll \mathcal{E}_{iz}$ and $v_e \propto \sqrt{T_e}$, as

$$\frac{\exp(\mathcal{E}_{iz}/T_e)}{\sqrt{T_e}} \propto (Rp)^2, \tag{9}$$

where the constant of proportionality depends on the type of gas. So for a given gas (given $\mathcal{E}_{iz}$ and M_i), the electron temperature is a unique function of the pressure radius product and is independent of the plasma density or discharge current. This relation is valid only when the electron mean free path is small compared to the tube radius.

The longitudinal electric field E is required to maintain the current in the presence of the diffusion losses. To determine the electric field, we apply the power balance. The ohmic power absorbed is given by

$$P_{abs} = 2\pi \int_0^R \mathbf{J} \cdot \mathbf{E} r \, dr \tag{10}$$

and the power lost due to the ion loss at the tube walls

$$P_{loss} = 2\pi R \Gamma_r e\mathcal{E}_T, \tag{11}$$

where $e\mathcal{E}_T = e(\mathcal{E}_c + \mathcal{E}_i + \mathcal{E}_e)$ is the total energy lost per electron–ion pair created, and $\mathcal{E}_i + \mathcal{E}_e$ is the kinetic energy lost to the wall per electron–ion pair lost to the wall. For a Maxwellian electron energy distribution and an insulating wall, $\mathcal{E}_i + \mathcal{E}_e = \frac{1}{2}T_e \ln(M_i/2\pi m_e) + 2T_e$. $\mathcal{E}_c$ is the collisional loss per electron–ion pair created

$$\mathcal{E}_c = \mathcal{E}_{iz} + \sum_i \mathcal{E}_{ex,i}\frac{k_{ex,i}}{k_{iz}} + \frac{k_{el}}{k_{iz}}\frac{3m_e}{M_i}T_e, \tag{12}$$

where $\mathcal{E}_{iz}$ is the ionization energy, $\mathcal{E}_{ex,i}$ and $k_{ex,i}$ are the excitation energy and rate coefficient for the ith excitation process, respectively, k_{el} is the elastic scattering rate coefficient. The electric field along the column can be determined by equating the absorbed and lost power and, substituting the radial density solution (equation (6)), we have

$$en_0 \mu_e E^2 2\pi \int_0^R J_0\left(r\sqrt{\frac{\nu_{iz}}{D_a}}\right) r \, dr$$
$$= 2\pi R(D_a \nu_{iz})^{1/2} n_0 J_1\left(R\sqrt{\frac{\nu_{iz}}{D_a}}\right)e\mathcal{E}_T, \tag{13}$$

where a constant mobility $\mu_e = e/m_e\nu_m$, and constant electric field are assumed, where m_e is the electron mass, $\nu_m = k_m n_g$ is the electron neutral collision frequency, k_m is the electron neutral collision rate coefficient (depends on T_e), and the current density

$$J = en\mu_e E \tag{14}$$

has been substituted. Performing the integration and solve for E gives

$$E = \left(\frac{\nu_{iz}\mathcal{E}_T}{\mu_e}\right)^{1/2} = \left(\frac{m_e}{e}\nu_{iz}\nu_m\mathcal{E}_T\right)^{1/2}, \tag{15}$$

where the electron mobility μ_e has been substituted. This can be written as

$$\frac{E}{n_g} = \left(\frac{m_e}{e}k_{iz}k_m\mathcal{E}_T\right)^{1/2}, \tag{16}$$

where the right-hand side only depends on the type of gas and the electron temperature. For a fixed pressure-radius product, the longitudinal electric field, and hence the voltage drop along a discharge, is fixed and is independent of the discharge current. Even though the analysis is somewhat oversimplified, this conclusion is mostly valid for many diffusion controlled positive column discharges. We can eliminate ν_{iz} using

equation (7) to obtain

$$E = \frac{\chi_{01}}{R}\left(\frac{D_a \mathcal{E}_T}{\mu_e}\right)^{1/2} = \frac{\chi_{01}}{R}\left(\frac{m_e k_m}{M_i k_{mi}}\mathcal{E}_T T_e\right)^{1/2}, \qquad (17)$$

where we have also substituted the ambipolar diffusion coefficient. Equation (17) indicates that the electric field depends only on T_e and is independent of the neutral gas pressure. As noted above, we need to determine the axial plasma density n_0. Integrating equation (14) over the discharge cross section then gives the current

$$I = 2\pi e n_0 \left(\frac{R^2}{\chi_{01}}\right) J_1(\chi_{01})\mu_e E \qquad (18)$$

which for a given discharge current and the electric field given by equation (17) gives the axial plasma density n_0. We note that equations (16) and (17) suggest that the electric field is independent of the discharge current, whereas measurements usually show that the electric field E decreases with increasing discharge current (Ingold 1978). This is called the negative voltage–current curve and it has been related to significant and increasing energy transfer from electrons to neutrals via elastic collisions as the current density is increased. Thus, the gas temperature is higher and the neutral gas density lower in the discharge center than at the tube wall, leading to higher electron mobilty in the discharge center (Ecker and Zöller 1964). Another mechanism that could lead to a negative voltage–current curve in the positive column is multistep ionization.

In reality, the electron energy distribution is not Maxwellian, there are higher average electron energies near the column edge, one step ionization is typically not the only path for ionization, and there is a significant radial variation in the average energy of the electrons in these discharges (Uhrlandt and Winkler 1996). The local approach is valid only for small values of pL, where the electron energy distribution is close to being Maxwellian.

For higher values of pL, the average electron energy can be significantly higher near the plasma edge than in the discharge center. This is because the colder electrons are confined by the potential in the discharge center while the higher energy electrons can overcome the potential energy hill. However, a full kinetic treatment, including the radial density variation is rather complicated. Instead various approximate kinetic methods have been employed to explore the positive column. One such method is the non-local approximation, originally suggested by Bernstein and Holstein (1954). The non-local approximation is an efficient method for the solution of the spatially dependent Boltzmann equation, but it is valid only in the limiting case that the energy relaxation length of electrons exceeds the discharge dimensions (Bernstein and Holstein 1954, Busch and Kortshagen 1995, Tsendin 1995). This indicates that the pressure has to be low. This method assumes that the total electron energy can be assumed constant and the entire electron kinetics can be described by a single, spatially homogeneous distribution of total electron energy which is determined from a spatially averaged kinetic equation.

Then the average energy, transport coefficients and collision frequencies can vary radially across the positive column even though the axial field does not. The non-local moment method is described by Ingold (1997) and compared to other approaches that can be extended to higher pressure regimes. They also state that the properties of the positive column at any pressure can be described adequately by moment equations, if the radial heat flow in the electron gas is taken into account, and when the electron transport coefficients and the relevant collision frequencies are allowed to depend on the radially varying average energy. Particle-in-cell simulation of the positive column show that the radial electron heat flow plays a major role in maintaining the global power balance in low pressure positive column discharge (Kawamura and Ingold 2001).

A tutorial on fluid modeling of the positive column of dc glow discharges was recently given by Alves (2007). There it is described how the electron transport parameters and rate coefficients are calculated using a local mean energy approximation along with a two-term Boltzmann solver. The obtained results allow to study the discharge energy deposition features in radial direction, as a function of pressure and axial current, along with the analysis of the space-charge sheath formation. The results show that the electron mean energy is almost constant in the plasma bulk, exhibiting a strong decrease near the discharge wall, following the electron density profile. The power balance in the bulk is dominated by Joule heating and by collisions across the discharge, while in the sheath, the power is balanced by the power lost in maintaining the space-charge field and the power gained from convection.

3.2. Striations

The positive column sometimes shows distinct and regular luminous bands along its length, that can be either moving or stationary, referred to as striations (Pekarek 1968, Raizer 1991, Kolobov 2006). Stratification of the positive column in a dc glow discharges into alternating bright and dark areas is a well-studied phenomenon, first time observed by Michael Faraday in the 1830s. These are due to fluctuations in the electron and ion density. The striation consists of a bright region, with a predominant generation of charged particles due to ionization, and a dark region were particle loss due to ambipolar escape to the discharge tube walls, and attachment to gas molecules and recombination in electronegative gas, is predominant. For the operation of the discharge at low pressure, the stratified state is energetically favorable, because for a given discharge current the voltage drop and the power dissipated in the positive column when striations are present are lower than in the uniform discharge (Raizer 1991, section 9.7).

The *standing striations* can be observed by the naked eye in molecular gases (such as hydrogen, nitrogen, oxygen) and in mixtures of molecular and rare gases (Lisovskiy *et al* 2012). Such stationary striations can be seen in figures 4 and 6. In pure rare gases, standing striations exist in the form of damping oscillations in front of cathode. *Moving striations* are traveling waves in the electron density. The moving
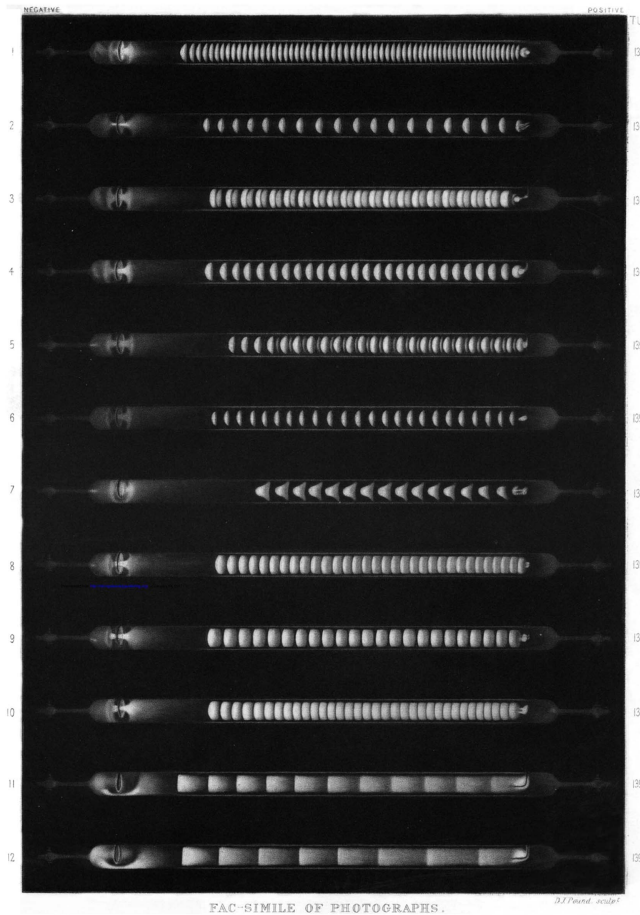
Figure 6. Photograph of standing striations in a low pressure dc glow discharge tube. The cathode is on the left and the anode is on the right. Reproduced with permission from de la Rue and Müller (1878).

striations typically exhibit frequencies in the range from a few Hz up to several tens of kHz. Moving striations cannot be observed by the naked eye due to their large velocity and require phase sensitive stroboscopic methods to be observed. In molecular gases, they usually move from cathode towards anode. Moving striations are discussed by Oleson and Cooper (1968).

Striations can be observed in a limited range of current values, gas type, gas pressure, and tube radius. Garscadden (1978) discussed the ranges of occurrence for various gases and operating conditions. Moving striations occur at low pressures, where the ionization mean free paths are long, longer or comparable to the density gradient scale length of the gas. Thus, Fick's law may not be valid. Watanabe and Oleson (1955) included both continuity and momentum equations for ions and electrons and the ion and electron densities are coupled through Poisson's equation. They demonstrated propagating ion density waves with phase velocity directed towards the cathode. Pekárek and Krejčí (1962) under the assumption of ambipolar diffusion used both the continuity and momentum equations along with Poissions equation and a simple energy balance equation. These analyses were summarized by Garscadden (1978).

4. The operation of the dc glow discharge

In the above discussion, we have used some terms like electrical breakdown and secondary electron emission. These phenomena are important in discharge physics and in particular for the operation of the dc discharge and will be explained briefly.

4.1. Vacuum breakdown

Electrical breakdown is an important phenomenon in discharge physics. Electrical breakdown is the process that describes the transition from a neutral gas to a self-sustained discharge. Thus, with the application of an electric field an electrically insulating gas transitions to a conducting state. The breakdown process is highly transient and a good time resolution imagning is required to study it. This kind of studies have been performed by Wagenaars *et al* (2005, 2006) who apply time reolved intensified charge-coupled device imaging to explore the breakdown process in low-pressure discharges, as well as direct measurements of the electric field strengths in ionization fronts during breakdown (Wagenaars *et al* 2007). They record a formation of a light emission region in front of the anode and then movement of this light front from the anode to the cathode as breakdown is initiated. The time scales involved in the breakdown process are mainly determined by the ion drift velocity (Wagenaars *et al* 2005). They explain this observation by a continuous electron avalanche developing in the discharge gap due to secondary electron emission from the cathode. This avalanche causes light emission due to excitation of the discharge gas and modification of the potential in the electrode gap due to a build-up of space charge. They conclude that the breakdown process is controlled by the development of multiple electron avalanches consistent with the standard view of Townsend breakdown into a glow discharge at low pressures. Here, we derive the breakdown voltage as a function of the product pL, the reduced electrode distance, the so called Paschen curve. Similar discussions can be found in various textbooks such as by Lieberman and Lichtenberg (2005, pp 457–63), Raizer (1991, chapter 7) and Roth (1995, section 8.6).

The electron density and flux grow exponentially from the cathode. Thus, the increase in the electron flux is proportional to the electron flux or

$$\frac{d\Gamma_e}{dz} = \alpha \Gamma_e, \tag{19}$$

where Γ_e is the electron flux and α, commonly expressing the number of ionization collisions per unit length by an electron or $\alpha(z) \equiv 1/\lambda_{iz}$, the inverse of the mean free path for ionization, and is known as Townsend's first ionization coefficient. The first Townsend coefficient or ionization coefficient is a complicated function of the accelerating field and gas pressure. The electron flux in the direction along the discharge axis (or the direction of the electric field) is then

$$\Gamma_e(z) = \Gamma_e(0) \exp\left[\int_0^z \alpha(z') dz' \right]. \tag{20}$$

Table 2. Constants for the Townsend ionization coefficient. The data is based on Lieberman and Lichtenberg (2005).

Gas	A $(\text{cm}^{-1}\,\text{Pa}^{-1})$	B $(\text{V cm}^{-1}\,\text{Pa}^{-1})$	Range of E/p $[\text{V cm}^{-1}\,\text{Pa}^{-1}]$
H_2	0.0360	1.0201	1.1251–3.0004
He	0.0210	0.5776	0.2250–1.8752
Ar	0.0862	1.3202	0.7501–4.5006
O_2	0.0488	1.4402	0.3750–0.9751
N_2	0.0885	2.4378	0.7501–4.5006
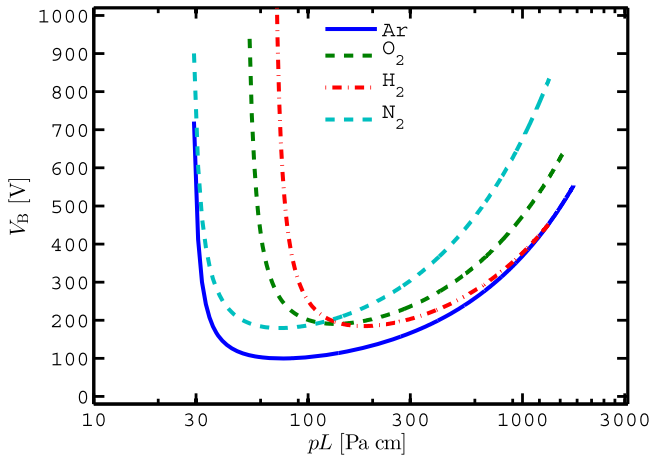
Figure 7. The breakdown voltage V_B versus the reduced electrode distance pL for a few common gases calculated using equation (26) and the data given in table 2, assuming $\gamma_{see} = 0.1$.

Due to continuity of the total charge (creation of equal numbers of electron–ion pairs) we can write

$$\Gamma_i(0) - \Gamma_i(L) = \Gamma_e(0)\left\{\exp\left[\int_0^L \alpha(z')\mathrm{d}z'\right] - 1\right\}, \quad (21)$$

where $\Gamma_e(L)$ from equation (20) has been inserted. Since the discharge must be self sustaining we have $\Gamma_e(0) = \gamma_{see}\Gamma_i(0)$ and $\Gamma_i(L) = 0$. Then

$$\exp\left[\int_0^L \alpha(z')\mathrm{d}z'\right] = 1 + \frac{1}{\gamma_{see}} \quad (22)$$

is the condition for self-sustainability. In a vacuum region, the electric field E is a constant and it follows that the electron drift velocity $\mu_e E$ is also a constant. Hence, the electron energy $\mathcal{E}_e$ is a constant, allowing us to treat α as a constant in equation (22). Taking the logarithm of both sides gives

$$\alpha L = \ln\left(1 + \frac{1}{\gamma_{see}}\right) \quad (23)$$

which is the breakdown condition for a dc discharge. The ionization coefficient is usually expressed in the form

$$\frac{\alpha}{p} = A\exp\left(-\frac{Bp}{E}\right), \quad (24)$$

where A and B are determined experimentally and found to be roughly constant over a range of pressures and fields for a

given gas type. The coefficients A and B for various common gases are listed in table 2.

If the minimum voltage of which the discharge initiates, the breakdown voltage, is written $V_B = EL$ then

$$ApL\exp\left(-\frac{BpL}{V_B}\right) = \ln\left(1 + \frac{1}{\gamma_{see}}\right) \quad (25)$$

which we solve for V_B to get

$$V_B = \frac{BpL}{\ln(ApL) - \ln\left[\ln(1 + 1/\gamma_{see})\right]} \quad (26)$$

which is a function of the product pL. The curve that shows V_B as a a function of the product pL is called the *Paschen curve* and is shown for a few common gases in figure 7. This curve shows that for a fixed discharge length L there is an optimum pressure for plasma breakdown. The Paschen curve is unique to each gas or gas mixture. At the lower pressures, the ionization process is ineffective due to the low electron–neutral collision probability while at higher pressures elastic collisions prevent the electrons from reaching high enough energy for ionization to occur. This behavior was first reported by de la Rue and Müller (1880) for discharges in hydrogen and air. The Paschen curve has been measured for dc discharges of various gases including nitrogen (Miller 1963, Lisovskiy *et al* 2000), argon (Lisovskiy *et al* 2000), carbon tetrafluoride (CF$_4$) (Lisovskiy *et al* 2015), and water vapor (Škoro *et al* 2011, Sivoš *et al* 2015).

In fact, the product of pressure and distance between the electrodes (pL) is the most suitable parameter to characterize the discharge. For instance, at lower pressure, the distance between cathode and anode has to be longer to create a discharge with properties comparable to those of high pressure with small distance between the electrodes. The number of gas atoms or molecules in the space between the electrodes is proportional to pL. For low pressure the electron mean free path is large, and most electrons reach the anode without colliding with gas atoms or molecules. Thus, the lower the pressure, the higher the value of V_B is required to generate enough electrons to cause the breakdown of the gas. At higher pressures, the electron mean free path is short. The electrons do not gain enough energy from the electric field to ionize the gas atoms or molecules due to their frequent collisions with the gas molecules. Therefore V_B increases as the pressure increases. To find the value of pL that corresponds to a minimum breakdown voltage, we differentiate the expression for the breakdown voltage, equation (26) with respect to pL and set the derivative equal to zero (Raizer 1991, chapter 7)

$$(pL)_{min} = \frac{\exp(1)}{A}\ln\left(1 + \frac{1}{\gamma_{see}}\right) \quad (27)$$

and the minimum voltage is then

$$V_{B,min} = \exp(1)\frac{B}{A}\ln\left(1 + \frac{1}{\gamma_{see}}\right) \quad (28)$$

and is referred to as the minimum sparking potential, and is the minimum voltage at which electrical breakdown can occur in a given gas. A low pressure dc glow discharge will adjust

the length of the cathode region such that a minimum value of the product pd_c is established

$$pd_c \approx (pL)_{\min} \tag{29}$$

which is the Paschen minimum given by equation (27).

Two discharges can be said to be similar if for equal applied voltages they carry equal currents, irrespective of their dimensions. The similarity principle states that when a given discharge A is operated under particular condition, a discharge B can be operated with the gas density of discharge A multiplied by a factor a and the linear dimensions multiplied by a factor $1/a$, then the space charge density and the current density scale by a factor a^2. So for similar discharges the requirement of equal currents leads to $\alpha_A L_A = \alpha_B L_B$, or $\alpha_B = \alpha_A/a$. Also, since V_D is the same for both discharges, $E_B = E_A/a$. Then the pressure scales as $p_B = p_A/a$ and we have $\alpha_B/p_B = (\alpha_A/a)/(p_A/a) = \alpha_A/p_A$ so α/p is invariant. Similarly, for similar discharges, pL_c is invariant, and E/p or E/n_g is invariant. The ratio E/p is a measure of the energy gain of a charged particle between collisions, and is referred to as the reduced electric field. Typically, it was found that the breakdown conditions and the current growth depend only on scaling parameters E/n_g, and pL (Phelps 2001), such as in case of the Paschen curve. Additionally, the discharge voltage can be expressed as a function of the reduced current density J/p^2, and Škoro *et al* (2008) have shown that the J/p^2 scaling law can be used to recognize the transition between different plasma regimes, from Townsend discharge, to the normal glow, and further to the abnormal glow, similar to the V_D–I_D characteristic presented in figure 1.

4.2. Secondary electrons

The emission of secondary electrons as a result of ion or neutral bombardment of a metallic surface plays an important role in the discharge physics. Typical energy of emitted electrons leaving the cathode surface is about few eV. Since the cathodes are held at negative potentials, the secondary electrons are accelerated away from the cathode surface with an energy equal to the potential drop ion the cathode sheath. These electrons sustain the discharge by ionization of the neutral gas, and generation of ions which then bombard the cathode releasing more secondary electrons. Ion- and neutral-induced secondary electron emission has been studied both theoretically and experimentally for decades (Parilis and Kishinevskii 1960, Abroyan *et al* 1967, Hasselkamp 1992).

The secondary electron emission yield or coefficient γ_{see} is defined as the number of secondary electrons emitted per incident ion or neutral. For low energies of impinging ion, the secondary electron emission yield is independent of the velocity of the bombarding particle, since the electron emission occurs due to transfer of the incoming ion or atom's potential energy to an electron in the cathode surface. This constant secondary electron emission yield is attributed to an Auger process referred to as *potential emission*. For impinging ion or neutral energies above several hundreds eV to keV the energy dependent portion of the yields is called *kinetic emission*. Kinetic emission, occurs when a bombarding

particle transfers sufficient kinetic energy to an electron in the cathode, starts contributing to the total yield at a threshold energy of around a few hundred electron volts and dominates at higher energies. Both experimental data and theory predict a linear dependence of the secondary electron emission yield on the bombarding energy close to the threshold energy, and linear dependence on the bombarding velocity at higher energies (Parilis and Kishinevskii 1960, Abroyan *et al* 1967, Cawthron 1971, Baragiola *et al* 1979, Hasselkamp 1992). At much higher energies, experimental data shows that the electron yield starts decreasing with increasing bombarding velocity. This occurs for a bombarding energy of around 100 keV for H^+ (Hasselkamp 1992).

The two different mechanisms are considered to be co-existing, so the total electron emission yield is written as

$$\gamma_{\text{see}} = \gamma_p + \gamma_k, \tag{30}$$

where γ_p and γ_k are the contributions from potential and kinetic emission to the total yield, respectively. In addition to the energy of the impacting particle, the secondary electron emission yield depends on the cathode material, but rarely exceeds 0.2 for an ion energy below 1 keV. The condition of the cathode significantly affects the ion induced secondary electron emission yield. Clean metals, i.e. metals free of oxidation, gas adsorption, and other contamination, generally have a lower kinetic emission yield than contaminated metals (Phelps and Petrović 1999). Phelps *et al* (Phelps and Petrović 1999, Phelps *et al* 1999) give the secondary electron emission yield in the energy range 10–10000 eV for both clean and dirty metal surfaces bombarded by Ar^+-ions and Ar neutrals.

4.3. The cathode sheath

All plasmas are separated from the surrounding walls by a sheath. The sheath properties determine the energy and flux of charged particles that bombard the wall surface. We have seen in section 3, and in particular in figure 5(a), that most of the potential drop over a dc glow discharge is across the cathode sheath. The relation between the current density, the voltage drop across the sheath and the sheath thickness was derived by Child (1911), assuming that the initial ion energy is negligible compared to the sheath potential (see also Lieberman and Lichtenberg (2005, section 6.2)), giving

$$J = \frac{4}{9}\epsilon_0\left(\frac{2e}{M_i}\right)^{1/2}\frac{V_c^{3/2}}{d_c^2} \tag{31}$$

which is called the Child law or the *collisionless Child–Langmuir law*. The Child law is valid when the sheath potential is large compared to the average energy of the electrons. A similar relation was derived by Langmuir (1913) for electrons emitted from a hot cathode approaching a cold anode.

In the *collisional* regime, where the pressure is high enough that the charged species interact frequently with neutral gas species, we can assume that the ion–neutral mean free path λ_i is independent of the ion velocity (Lieberman and Lichtenberg 2005, section 6.6). This gives the collisional

Child law

$$J = \left(\frac{2}{3}\right)\left(\frac{5}{3}\right)^{3/2} \epsilon_0 \left(\frac{2e\lambda_i}{\pi M_i}\right)^{1/2} \frac{V_c^{3/2}}{d_c^{5/2}}. \tag{32}$$

Alternatively, assuming that diffusion of ions is negligible compared to drift due to electric field and take the ion mobility μ_i to be independent of the ion velocity to get

$$J = \frac{9}{8} \epsilon_0 \mu_i \frac{V_c^2}{d_c^3} \tag{33}$$

which is referred to as the Mott–Gurney law. It was derived to describe the current at the interface of a semiconductor and insulator (Mott and Gurney 1948, chapter V) and later adapted to describe the current through the discharge sheath by Cobine (1958). Equation (33) is valid only at very high pressures (low drift velocities). We note here that the scalings of the current density with both V_c and d_c in equation (32) are different from equation (33). Further discussion of the collisionless Child–Langmuir law and the collisional Mott–Gurney law is given by Benilov (2009). It has been demonstrated by experiments that the Mott–Gurney law (equation (33)) applies to a dc glow discharge in hydrogen (Lisovskiy et al 2016) and nitrogen (Lisovskiy et al 2014) for most of the pressure range from 10 to 333 Pa.

5. The dc glow discharge sputtering source

An important process that can occur at the cathode in the glow discharge is sputtering, which is ejection of the atoms from the cathode surface by the impinging ions. Sputtering can occur if the voltage applied to the cathode is sufficiently high. When the ions and fast neutrals from the plasma bombard the cathode target, they release secondary electrons and they also release atoms of the cathode material.

5.1. Sputter yield

Sputtering is the ejection of atoms due to bombardment of a solid or a liquid surface (the target) by energetic particles, often ions (Behrisch and Eckstein 2007). When the cathode surface is struck by an impinging particle in a given energy range some atoms in the surface, referred to as primary knock on atoms, may gain substantial amount of the energy of the incoming ion through the collision. They in turn sputter or strike other atoms in the surface transferring momentum yet again (Behrisch and Wittmaack 1991). The sputter yield also depends on the ion incident angle. The sputter yield increases with increasing angle of incidence and maximum occurs in the range between $60°$ and $80°$ (Oechsner 1975).

The sputter yield Y is defined as the mean number of atoms removed from the target surface for each incident ion. The maximum transferable energy in a collision has to be larger than the surface binding energy or $\mathcal{E}_{th} + \mathcal{E}_{sp} > \mathcal{E}_{sb}/\Lambda$ where $\mathcal{E}_{sb}$ is the surface binding energy (heat of sublimation) of the target material, $\mathcal{E}_{sp}$ is the binding energy of a projectile to the target surface ($\mathcal{E}_{sp} = 0$ for noble gas ions) and

$\Lambda = 4M_i M_t/(M_i + M_t)^2$ is the energy transfer factor in a binary collision and M_i and M_t are the masses of the projectile and the target atom, respectively (Eckstein 2007). The minimum ion energy required for sputtering to take place is known as the threshold energy for sputtering and is given by (Yamamura and Tawara 1996)

$$\mathcal{E}_{th} = \begin{cases} \mathcal{E}_{sb}\left(1 + 5.7\dfrac{M_i}{M_t}\right)\Big/\Lambda & \text{if} \quad M_i \leqslant M_t. \\ \mathcal{E}_{sb} \times 6.7/\Lambda & \text{if} \quad M_i \geqslant M_t \end{cases} \tag{34}$$

Yamamura and Tawara (1996) give the various empirical formulas for the sputter yield as a function of ion bombarding energy and data for various combinations of ions and target materials. In the energy range of interest here, 20–5000 eV, the sputter yield increases with increasing incident ion energy. In this energy range, the sputter yield can be approximated by

$$Y(\mathcal{E}_i) = a\mathcal{E}_i^b \tag{35}$$

where a, a material dependent parameter, and $b \sim 0.5$ are fit parameters that are given for a particular combination of bombarding ion and target materials (Anders 2017). As an example for Ar^+ bombarding, a Cu target $a = 0.1421$ and $b = 0.468$, while for the self-sputtering Cu^+ bombarding a Cu target $a = 0.0691$ and $b = 0.556$.

Computer codes such as TRIM (transport of ions in matter) (Biersack and Haggmark 1980), SRIM (stopping and range of ions in matter) (Ziegler et al 2008, 2010) and TRI-DYN (a TRIM simulation code including dynamic composition changes) (Möller and Eckstein 1984, Möller et al 1988) are used to calculate the sputter yield for a given inpacting species as a function of the energy of the incident particle. They use a binary collision model and follow the incident particles and all of its cascade atoms until they sputter or their energy is too low to escape the surface potential.

5.2. Energy distribution of sputtered atoms

The atoms sputtered off the cathode target are considerably more energetic than thermally evaporated atoms (a few eV as compared to about a tenth of an eV). Usually it is desirable to maintain this initial kinetic energy of the sputtered atoms, since it has favorable effects on the film growth (Petrov et al 1993). Relatively low pressures are normally desired to minimize scattering of the sputtered atoms. The sputtering process is, therefore, normally a line-of-sight process where the deposition flux cannot be easily controlled, since it consists of neutral atoms. A broad distribution has been measured for sputtered neutrals (Stuart et al 1969) and is predicted by the Thompson random collision cascade model (Thompson 1968, 1981). According to the Sigmund–Thompson theory, the energy distribution function can be approximated by

$$f_{S-T} \propto \frac{\mathcal{E}}{(\mathcal{E} + \mathcal{E}_{sb})^{3-2m}}, \tag{36}$$

where $\mathcal{E}_{sb}$ is the binding energy of the target material and m is the exponent in the interaction potential applied

$V(r) \propto r^{-m}$ (Hofer [1991]). Often m is taken to be 0.2. This model predicts an energy spectrum that peaks sharply at $\frac{1}{2}\mathcal{E}_{sb}$, followed by a gradual decrease to higher energies ($\propto 1/\mathcal{E}^2$). The energy distribution of atoms ejected from a target is expected to be independent of the nature of the incident ion as well as the crystal structure of the target. The angular distribution of the sputtered atoms is often described as a cosine distribution. That says that the relative amount of material sputtered at any particular angle can be compared to the amount sputtered at normal incidence times the cosine of the angle from normal incidence. This means that the overall distribution can be drawn as a ellipse, and in three dimensions, the distribution would appear as an ellipsoid centered on the ion impact point. For a more detailed discussion of the ion energy and ion angular distribution of the sputtered material, the reader should consult the reviews given by Hofer ([1991]) and Gnaser ([2007]) or the original work of Thompson ([1968], [1981]) and Sigmund ([1969]).

If the sputtered material is subsequently ionized, the ion energy distribution generally shows a narrow low energy peak, due to thermalized atoms which are accelerated by the difference between plasma potential (several eV) and grounded electrode, and a broad distribution at higher energies, which originates from the sputtered neutrals which have been ionized by electron impact within the plasma (see e.g. Andersson *et al* [2006]). Due to the small mass of the electron the electron impact ionization does not change the energy of the resulting ion by much.

5.3. Diode sputtering

Sputtering in gas discharges was discovered in the mid 19th century (Grove [1852]), while film formation utilizing sputter deposition was first reported by Wright ([1877a], [1877b]) a few decades later. Sputtering of thin films had already found commercial application by the 1930s (Fruth [1932]) but gained significant interest in the late 1950s and early 1960s with improved vacuum technology and the realization that a wide range of materials could be deposited using sputtering (Kay [1962], Westwood [1976], Thornton and Greene [1994]) including dielectrics, but then by applying rf voltage (Anderson *et al* [1962]). There have been a number of review articles and books covering dc glow discharge sputter deposition (Kay [1962], Chopra [1969], Westwood [1976], Vossen and Cuomo [1978]).

For decades, the dc glow discharge was used as a sputter source, commonly referred to as diode sputtering. A schematic of the diode sputter arrangement is shown in figure [8]. The distance between cathode and anode is generally short, so typically only a short anode zone is present together with the cathode dark space and the negative glow, where the slightly positive plasma potential returns back to zero at the anode. They are often low aspect ratio, the interelectrode separation is small compared to the size of the electrode, ($L/R < 1$ for a cylindrical configuration) and mainly used for sputtering of metals. The cathode serves as a target for ion impact sputtering and is the material source. Cathode diameters are
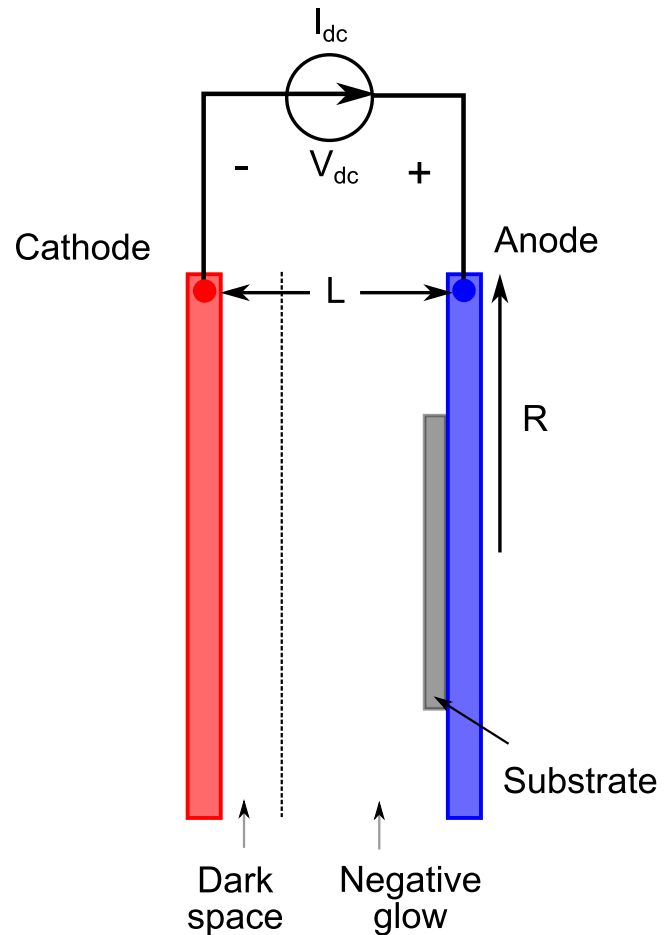
Figure 8. Low aspect ratio dc glow discharge used for sputtering or the dc diode sputter source. The cathode is the material source. The interelectrode separation is a few times that of the cathode dark space and the negative glow extends almost to the anode. The substrate is placed on the anode.

typically in the range 10–30 cm while the spacing between the cathode and anode is 5–10 cm. The interelectrode separation is a few times that of the cathode dark space. This configuration is referred to as an obstructed dc glow discharge. If the length of a glow discharge is less than L_c at the Paschen minimum value given by equation ([29]), then the voltage drop over the cathode fall rises above the Paschen minimum value, $V_{c,min}$. Almost all the voltage appears across cathode sheath (dark space, i.e. cathode fall). The negative glow extends almost to the anode and the positive column is commonly absent in these short discharges. Typical dc glow discharge for sputter deposition requires a negatively charged cathode at 2000–5000 V and a grounded surface anode. The substrate holder may be grounded, floating, biased, heated, cooled, or some combination of these.

In the dc sputtering diode configuration, the ions that impinge on the target surface do not have the full cathode fall potential. This is due to the collisional sheath (equations ([13]) and ([14])) where the working gas pressure is high enough to allow charge-exchange collisions and momentum transfer
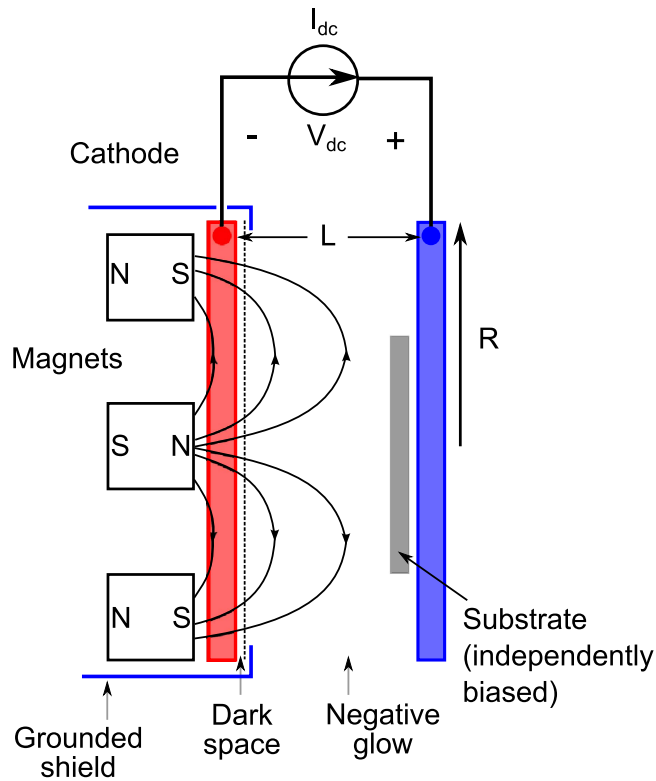
Figure 9. A schematic of the dc planar magnetron discharge used for sputtering. Permanent magnets behind the cathode target confine the secondary electrons in the vicinity of the target surface. The anode is often a grounded shield around the magnetron target.

collisions (thermalization) between the accelerating ions and the working gas neutrals. The consequence is that there is a broad energy spectrum of ions and high energy neutrals that impinge on the target surface. The higher the gas pressure, the lower the mean energy of particles that bombard the target. Since the discharge is maintained by secondary electron emission the operating pressure must be high enough so that the secondary electrons are not lost to the anode or to the grounded surfaces before performing ionization. These pressures are higher than preferred for optimum transport of the sputtered deposition atoms due to scattering by the gas atoms. Hence, there is a narrow pressure range around 2–4 Pa for dc glow discharge sputtering to be viable. At this pressure the cathode dark space extends about 1–2 cm from the cathode. The discharge maximum current density is roughly $1\,\text{mA cm}^{-2}$ and the deposition rate ten nm min^{-1} at best. The dc sputter source is generally weekly ionized with ionization fraction of the order of 10^{-4}. Furthermore, a conventional dc diode discharge is not operable if the cathode surface is insulating. This would be the case if the cathode was itself an insulator, or if the cathode was under operation in reactive gas such as oxygen which might make the surface of the cathode insulating. This results in either case in extremely low discharge currents and very low sputtering rate.

The disadvantages of dc diode sputter deposition include low sputtering rate, target poisoning by reactive contaminants, surface heating due to electrons accelerated away from the target, and that only electrical conductors can

be used as sputtering targets. Also the sputtering power efficiency (sputtered atoms/ion-volt) is relatively low in these discharges as they operate at high voltage and this efficiency decreases with increasing energy.

6. The magnetron sputtering discharge

The high discharge voltage and high operating pressure of dc discharge sputtering source are limiting to its application. In order to lower the discharge voltage and expand the operation pressure range, the lifetime of the electrons in the target vicinity had to increase in order to enhance the ionization. This was achieved by applying a static magnetic field applied to confine the secondary electrons in the vicinity of the cathode target (Gill and Kay 1965, Wasa and Hayakawa 1969). This is referred to as a magnetron sputtering discharge. With the introduction of magnetron sputtering the disadvantages of diode sputtering, such as poor deposition rate, were overcome as the operating pressure could be reduced, while maintaining the energy of the sputtered species, often resulting in improved film properties. A schematic of a dc planar magnetron sputtering configuration is shown in figure 9. In the planar configuration, the magnetron sputtering discharge is simply a diode sputtering arrangement with the addition of magnets directly behind the cathode. The magnetic field lines go out in the center of the cathode and go back into the cathode at the annular (Chapin 1974, Waits 1978). The magnetic field is arranged so that it appears parallel to the cathode surface. In a conventional dc magnetron sputtering (dcMS) discharge, the cathode is kept at a constant negative voltage. Sometimes a planar magnetron discharge consists of a planar cathode (sputtering source or target) parallel to an anode surface. However, in most cases the anode is the grounded shield around the magnetron target (as seen in figure 9).

A simple model that gives an estimate of the minimum voltage needed to sustain a magnetron sputtering discharge was set forth by Thornton (1978). The number of electron–ion pairs created by each secondary electron that is trapped in the target vicinity is given as

$$\mathcal{N} \approx \frac{V_{\text{d}}}{\mathcal{E}_{\text{c}}}, \tag{37}$$

where $\mathcal{E}_{\text{c}}$ is the energy loss per electron–ion pair created with the flow of secondary electrons into the plasma as the source of energy (Thornton 1978, Thornton and Penfold 1978, Lieberman and Lichtenberg 2005, Depla *et al* 2010). For argon and high energy electrons, $\mathcal{E}_{\text{c}} \approx 20$ V. However, not all the secondary electrons are confined in the target vicinity. To account for the electrons that are not trapped, we define an effective secondary electron emission coefficient

$$\gamma_{\text{see,eff}} = m\epsilon_{\text{e}}(1 - r)\gamma_{\text{see}},$$

where ϵ_{e} is the fraction of the electron energy that is used for ionization before being lost, m is a factor that accounts for secondary electrons ionizing in the sheath and r is the recapture probability of secondary electrons. To sustain the

discharge, the condition

$$\gamma_{\mathrm{see,eff}} \mathcal{N} = 1 \tag{38}$$

has to be fulfilled. This defines the minimum voltage to sustain the discharge as

$$V_{\mathrm{D,min}} = \frac{\mathcal{E}_{\mathrm{c}}}{\beta \gamma_{\mathrm{see,eff}}} \tag{39}$$

where β is the fraction of ions that return to the cathode. Equation (39) is often referred to as the Thornton equation. The basic assumption is that acceleration across the sheath is the main source of energy for the electrons (Thornton 1978). Above breakdown, the parameters m, β, ϵ_{e} and r can vary with the applied voltage, so we can rewrite the Thornton equation for any voltage as (Depla *et al* 2009)

$$\frac{1}{V_{\mathrm{D}}} = \frac{\beta m \epsilon_{\mathrm{e}}(1 - r)}{\mathcal{E}_{\mathrm{c}}} \gamma_{\mathrm{see}}. \tag{40}$$

Thus, a plot of the inverse discharge voltage $1/V_{\mathrm{D}}$ against γ_{see} should then give a straight line through the origin. However, there are indications that the magnetron sputtering discharge is not fully maintained by acceleration of secondary electrons emitted from the cathode target. When experimentally determined $1/V_{\mathrm{D}}$ is plotted against γ_{see}, it does not go through the origin (Depla *et al* 2009). This suggests that Ohmic heating within the dense plasma, which hovers next to the cathode surface, seems to play a significant role as well (Brenning *et al* 2016).

The main advantage of the planar magnetron is that the sputtered material is transported in the direction normal to the cathode plane and will uniformly coat a surface that is translated past the magnetron target. Conventional planar dcMS sources are commonly operated using argon as the working gas in the pressure range 0.1–1.5 Pa and the applied cathode voltage in the range of 300–700 V. This leads to current densities of the order of 4–60 mA cm^{-2} and power densities of several tens of W cm^{-2} (Waits 1978). Magnetron sputtering configurations use a magnetic field ($\sim$20–50 mT), usually from permanent magnets near the target (cathode) surface, to confine the electrons near the surface. The electron density in the substrate vicinity is typically in the range 10^{15}–10^{17} m^{-3}. The static deposition rate is in the range 20–200 nm min^{-1}. The degree of ionization of the sputtered material is generally very low, often on the order of 1% or less. The majority of the ions bombarding the substrate are ions of the working gas as the mean free path for the sputtered material with respect to electron impact ionization is over 50 cm.

It is referred to as a balanced planar magnetron, when an axisymmetric magnetic field is applied with a permanent magnet behind the cathode, in such a way that the magnetic field lines start and return at the magnet. To increase the ion flux to the substrate, the magnetic field lines can be configured such that they do not all close at the cathode surface. This is referred to as unbalanced magnetron sources (Window and Savvides 1986). Then some of the electrons are lead towards the substrate, and by ambipolar diffusion, ions as well. Hence, by altering the magnetic field configuration, thin film growth can be achieved with varying ion and electron flux.

In the rotatable cylindrical magnetron sputtering discharge, the magnet assembly is installed inside the cylindrical cathode target (Wright and Beardow 1986). The target can rotate during the sputtering so it erodes uniformly and the target utilization is as high as 90%. This configuration also allows for deposition on large area substrates. In the cylindrical configuration, the target surface area may be in hundreds and up to tens of thousands of square cm. These rotatable targets are essential for deposition on large area glass for architectural and automotive applications, as well as for the production of flat panel displays and photovoltaic solar cells (Blondeel *et al* 2009).

6.1. Pulsed magnetron sputtering discharges

The asymmetric bipolar dc sputtering discharge was developed to optimize the deposition of insulating films from conductive targets with reactive sputtering (Schiller *et al* 1993, Sellers 1998). Pulsing the magnetron discharge in the medium frequency range (10–250 kHz) when depositing insulating films can significantly reduce the formation of arcs and, consequently, reduce the number of defects in the resulting film. In asymmetric bipolar mode, the target is pulsed between the normal operating voltage and a slightly positive (roughly 10%–20% of the negative voltage amplitude) voltage for a short duration.

More recently high-power pulsed magnetrons in unipolar mode have been proposed for highly ionized sputtering (Gudmundsson *et al* 2012). High power impulse magnetron sputtering is a sputtering technique where a high density plasma is created by applying high power pulses at low frequency and low duty cycle to a magnetron sputtering device. Then the peak electron density is in the range of 10^{18}–10^{19} m^{-3} which corresponds to an electron impact ionization mean free path for the sputtered material of the order of 1 cm or less. Thus, the sputtered material is highly ionized. For the ionized material, the ion energy as well as the ion flux can easily be controlled over a wide range making it possible to tailor phases, microstructure, defect density, and composition of growing film as well as utilizing the metal ions for etching (Helmersson *et al* 2006). Furthermore, as the sputtered material is ionized it enables guiding and aligning of the deposition material.

7. Chemical analysis with glow discharges

Low pressure glow discharges constitute a standard method for chemical analysis of metals and metallurgical samples. This method is referred to as glow discharge optical emission spectrometry (GD-OES) and is currently a well established technique in particular for surface and interface characterization (Broekaert 2003, Nelis and Payling 2003). The method was suggested by Grimm in the late sixties (Grimm 1968) for bulk analysis of solid conducting samples. Later, it was developed into allowing for quantitative depth

profiling of surfaces and coatings (Pons-Corbeau 1985). By applying radio frequency, the analysis of insulating materials was made possible (Duckworth and Marcus 1989). The sample to be analyzed is mounted on an o-ring on the outside of the plasma source, so that sample placement is rather easy and simple. Argon gas is introduced into the chamber of roughly 200–500 Pa. As voltage is applied to the sample, which is the cathode, a glow discharge is created and sputtering is initiated. The plasma forms in a hollow anode glow discharge. The glow discharge is connected to an optical spectrometer. The recorded intensity of an atomic emission line is a measure of the number of atoms of a particular element in the plasma and thus the concentration of the element in the sample analyzed. Glow discharge atomic emission spectra have narrow lines as a result of the low Doppler and pressure broadening. Analytical glow discharges are typically operated as abnormal glow discharges.

Similarly, mass spectrometry can also be applied for elemental analysis of solids, and then the process is referred to as glow discharge mass spectrometry (Coburn and Harrison 1981, Harrison *et al* 2003). Then a mass spectrometer is attached to the discharge and the ions of the material sputtered off the sample are sampled through an orifice. One advantage of elemental mass spectrometry is that is permits easier quantitative interpretation over the line rich optical emission spectra. They also have the ability to obtain the full periodic table, including information on isotopes with detection limit that is 2–3 orders of magnitude better than OES. Also, another advantage is achieved by using a pulsed glow discharge that gives a temporal separation of discharge gas ions and the analyte ions, particularly with the application of a time-of-flight mass spectrometer.

8. The Penning discharge

In the Penning discharge, a strong axial magnetic field is applied to the dc discharge (Hooper 1969). They can operate at very low pressures since the electrons have a very long ionization mean free paths due to being magnetically confined. Penning discharges can provide energetic ions of any material that can be gasified. The early application of this arrangement of the electric and magnetic field was when Penning introduced a manometer for low gas pressures, for the pressure range of 0.01 mPa–0.01 Pa, consisting of a glow discharge tube in a magnetic field (Penning 1937). Its operation is based on the fact that the current through the discharge is proportional to the pressure. This manometer is very simple in use and gives an instantaneous indication of pressure. This concept is also utilized in a combination of homogeneous magnetic field and electrostatic quadrapole potential arranged in such a way that it can trap a single particle (Brown and Gabrielse 1986). This is know as a Penning trap. Electrons are initially introduced into the trap via field emission. This creates an electron beam that ionizes residual gas to produce slow electrons which are then

captured in the trap. Thus, it allows for measuring physical quantities of individual particles at very high precision.

9. Hollow cathode discharges

Hollow cathode discharges are gas discharges between a hollow structured cathode and an arbitrarily shaped anode. The hollow cathode cavity can present plane-parallel, cylindrical, or spherical geometry. The open side of the cathode faces the anode side of the discharge. The anode can be remote. The hollow cathode discharge is based on an entrapment of electrons inside the hollow cathode. The cathode walls are made of conducting, refractory materials kept at the cathode potential. When energetic electrons emitted from one cathode wall are accelerated across the sheath towards the opposite wall they reach an identical sheath on the opposite side with the same but opposite electric field and they are reflected back. Thus the electrons are trapped and forced to oscillate between the opposite sheaths. During these oscillations, electrons will undergo inelastic collisions with gas atoms and therefore increase the probability of ionization and leading to a very dense plasma inside the cathode volume. This mechanism is referred to as the hollow cathode effect (Kolobov and Tsendin 1995). The plasma existing at the inter-electrode space can penetrate the hollow cathode, thus assuring a strong interaction between the plasma and the cathode internal surface. The plasma created within the hollow cathode is then finally forced out of the cathode along with the flowing gas. For further information on hollow cathode discharges, the reader is referred to the reviews by Mavrodineanu (1984), Pillow (1981), Delcroix and Trindade (1974), and Muhl and Pérez (2015).

Hollow cathodes have been utilized in different discharge devices, working under varying conditions in widely extended ranges. Hollow cathode discharges are widely used as electron and ion sources and as a source of intense line radiation. Initially they were used as thermionic emitters to produce electron beams. The large area of the hollow cathode emitter lead to extended lifetime of the emitter surface. These were operated in high vacuum. But hollow cathodes are also operated as plasma discharges. The primary advantage of the hollow cathode discharge is that a high degree of ionization can be sustained, in the negative glow, even for a rare gas/metal vapor mixture.

Hollow cathodes are critical components of Hall thrusters where they provide the electrons that ionize the neutral propellant gas to create the plasma which is then directed to create thrust and supply the electrons that neutralize the exhaust ion beam in gridded ion thrusters (Goebel and Katz 2008, chapter 6). The currents drawn may be rather significant or up to 100 A. The hollow cathode discharges have also been used as sputter sources for sputter deposition (Muhl and Pérez 2015). The hollow cathode magnetron sputtering discharge is an example where a hollow cathode is combined with a dcMS discharge in order to achieve high ionization fraction of the deposition material (Klawuhn *et al* 2000).

9.1. Plasma display panels

Another common use of dc plasmas is in PDP. The PDP is based on small gas discharges: micro-discharges, to generate a basic color (red, green or blue) of a pixel. There are two predominant ways of limiting the current in PDPs; dc display current limiting, which is based on current-limiting properties of the system resistance, and the ac display current limiting, which is based on the capacitance generated by a dielectric glass layer of the plasma cell. More detailed discussion on PDPs can be found in the review articles given by Boeuf (2003) and Weber (1985).

The more commonly used ac PDP consists of two glass plates placed at a distance of 100–200 μm from each other. The region between the plates is filled with a gas at a pressure of roughly 60 kPa. The PDP discharge operates in glow discharge regime since the pL value of a such system is in range of several kPa cm. The lines of electrodes are placed on the outer sides of both glass plates, in such a way that the electrodes of one plate are placed perpendicular to the electrodes of the other plate in order to form the rows and columns of a display. At each intersection between a row and a column electrode, a discharge can be formed, independent of the other intersections, by applying suitable voltage pulses to the electrodes.

Each pixel consists of three plasma cells corresponding to three basic colors (red, green and blue). On one side the plasma cell is covered with a thin layer of phosphor (red, green, or blue) and on the other side with a thin layer of another material, typically magnesium oxide (MgO). The discharge gas is typically a mixture of rare gases (xenon/neon/helium) which emit UV photons. The UV radiation activates color phosphors and visible light is emitted from each pixel. The MgO layer is very important for efficiency and longevity of the cell; it has a large secondary electron yield (keeping the operating voltage relatively low), high transmission in the visible range, and good resistance to sputtering (long lifetime).

10. Summary

We have given an overview of the dc discharge and in particular the dc glow discharge. The dc discharge typically has a negative cathode at one end and a positive anode at the other end, separated by a gas filled gap, enclosed in a long glass cylinder. We discussed the current–voltage characteristics of the discharge, as well as the distinct structure that develops in the glow discharge region, for discharge current in the range from μA to mA at operating pressure of 0.5–300 Pa. The dc glow discharge exhibits a distinct structure and is maintained by the emission of secondary electron emission from the cathode target. The dc glow discharge has been used as a sputter source, often operated as an obstructed abnormal glow discharge and the required applied voltage is in the range 2–5 kV. The magnetron sputtering discharge was developed in order to lower the discharge voltage and expand the operation pressure. We also briefly discussed other configurations of the dc discharge including its use in chemical analysis of surfaces, the Penning discharge and the hollow cathode discharges.

Acknowledgments

ORCID iDs

Jon Tomas Gudmundsson ⬤ https://orcid.org/0000-0002-8153-3209
Ante Hecimovic ⬤ https://orcid.org/0000-0002-3281-8507

References

Abroyan I A, Eremeev M A and Petrov N N 1967 Excitation of electrons in solids by relatively slow atomic particles *Phys.—Usp.* **10** 332–67

Alves L L 2007 Fluid modelling of the positive column of direct-current glow discharges *Plasma Sources Sci. Technol.* **16** 557–69

Anders A 2017 Tutorial: reactive high power impulse magnetron sputtering (R-HiPIMS) *J. Appl. Phys.* **121** 171101

Anderson G S, Mayer W N and Wehner G K 1962 Sputtering of dielectrics by high-frequency fields *J. Appl. Phys.* **33** 2991–2

Andersson J M, Wallin E, Münger E P and Helmersson U 2006 Energy distributions of positive and negative ions during magnetron sputtering of an Al target in Ar/O$_2$ mixtures *J. Appl. Phys.* **100** 033305

Baragiola R A, Alonso E V, Ferron J and Oliva-Florio A 1979 Ion-induced electron emission from clean metals original research article *Surf. Sci.* **90** 240–55

Behrisch R and Eckstein W 2007 Introduction and overview *Sputtering by Particle Bombardment: Experiments and Computer Calculations from Threshold to MeV Energies (Topics in Applied Physics* vol 110) ed R Behrisch and W Eckstein (Berlin: Springer) ch 1, pp 1–10

Behrisch R and Wittmaack K 1991 Introduction *Sputtering by Particle Bombardment III (Topics in Applied Physics* vol 64) ed R Behrisch and K Wittmaack (Berlin: Springer) pp 1–13

Benilov M S 2009 The Child–Langmuir law and analytical theory of collisionless to collision-dominated sheaths *Plasma Sources Sci. Technol.* **18** 014005

Bernstein I B and Holstein T 1954 Electron energy distributions in stationary discharges *Phys. Rev.* **94** 1475–82

Biersack J P and Haggmark L G 1980 A Monte Carlo computer program for the transport of energetic ions in amorphous targets *Nucl. Instrum. Methods* **174** 257–69

Blondeel A, Persoone P and De Bosscher W 2009 Rotatable magnetron sputter technology for large area glass and web coating *Vak. Forsch. Prax.* **21** 6–13

Boeuf J P 2003 Plasma display panels: physics, recent developments and key issues *J. Phys. D: Appl. Phys.* **36** R53–79

Booth J P, Fadlallah M, Derouard J and Sadeghi N 1994 Electric field measurements in discharges by 2 + 1 photon laser Stark spectroscopy of atomic hydrogen *Appl. Phys. Lett.* **65** 819–21

Brenning N, Gudmundsson J T, Lundin D, Minea T, Raadu M A and Helmersson U 2016 The role of Ohmic heating in dc magnetron sputtering *Plasma Sources Sci.Technol.* **25** 065024

Broekaert J A C 2003 Optical emission spectrometry with glow discharges *Glow Discharge Plasmas in Analytical Spectroscopy* ed R K Marcus and J A C Broekaert (Chichester: Wiley) pp 15–69

Brown L S and Gabrielse G 1986 Geonium theory: physics of a single electron or ion in a Penning trap *Rev. Mod. Phys.* **58** 233–311

Brown S C 1978 A short history of gaseous electronics *Gaseous Electronics: Electrical Discharges* vol 1 ed M Hirsh and H J Oskam (New York: Academic) pp 1–18

Budtz-Jørgensen C V 2001 Studies of electrical plasma discharges *PhD Thesis* Aarhus University

Busch C and Kortshagen U 1995 Numerical solution of the spatially inhomogeneous Boltzmann equation and verification of the nonlocal approach for an argon plasma *Phys. Rev. E* **51** 280–8

Cawthron E R 1971 Secondary electron emission from solid surfaces bombarded by medium energy ions *Aust. J. Phys.* **24** 859–70

Chapin J S 1974 The planar magnetron *Research/Development* **25** 37–40

Cherrington B E 1979 *Gaseous electronics and gas lasers* (Oxford: Pergamon)

Child C D 1911 Discharge from hot CaO *Phys. Rev.* **32** 492–511

Chopra K L 1969 *Thin Film Phenomena* (New York: McGraw-Hill)

Cobine J D 1958 *Gaseous Conductors* (New York: Dover)

Coburn J W and Harrison W W 1981 Plasma sources in analytical mass spectrometry *Appl. Spectrosc. Rev.* **17** 95–164

de la Rue W and Müller H W 1878 Experimental researches on the electric discharge with the chloride of silver battery *Phil. Trans. R. Soc.* **169** 155–241

de la Rue W and Müller H W 1880 Experimental researches on the electric discharge with the chloride of silver battery *Phil. Trans. R. Soc. London* **171** 65–116

Delcroix J-L and Trindade A R 1974 Gas discharge displays: a critical review *Advances in Electronics and Electron Physics* vol 35 ed L Marton (New York: Academic) pp 87–190

Den Hartog E A, Doughty D A and Lawler J E 1988 Laser optogalvanic and fluorescence studies of the cathode region of a glow discharge *Phys. Rev. A* **38** 2471–91

Depla D, Mahieu S and De Gryse R 2009 Magnetron sputter deposition: linking discharge voltage with target properties *Thin Solid Films* **517** 2825–39

Depla D, Mahieu S and Greene J E 2010 Sputter deposition processes *Handbook of Deposition Technologies for Films and Coatings* ed P M Martin 3rd edn (Oxford: William Andrew) ch 5, pp 253–96

Doughty D A, Den Hartog E A and Lawler J E 1987 Current balance at the surface of a cold cathode *Phys. Rev. Lett.* **58** 2668–71

Doughty D K, Den Hartog E A and Lawler J E 1985 Optogalvanic measurements of gas temperature in the cathode fall *Appl. Phys. Lett.* **46** 352–4

Druyvesteyn M J and Penning F M 1940 The mechanism of electrical discharges in gases of low pressure *Rev. Mod. Phys.* **12** 87–174

Duckworth D C and Marcus R K 1989 Radio frequency powered glow discharge atomization/ionization source for solids mass spectrometry *Anal. Chem.* **61** 1879–86

Ecker G and Zöller O 1964 Thermally inhomogeneous plasma column *Phys. Fluids* **7** 1996–2000

Eckstein W 2007 Sputtering yields *Sputtering by Particle Bombardment: Experiments and Computer Calculations from Threshold to MeV Energies* (*Topics in Applied Physics* vol 110) ed R Behrisch and W Eckstein (Berlin: Springer) pp 33–187

Francis G 1956 The glow discharge at low pressure *Gas Discharges II / Gasentladungen II* (*Encyclopedia of Physics* vol 4) ed S Flügge (Berlin: Springer) pp 53–208

Fruth H F 1932 Cathode sputtering, a commercial application *Physics* **2** 280–8

Garscadden A 1978 Ionization waves in glow discharges *Gaseous Electronics: Electrical Discharges* vol 1 ed M Hirsh and H J Oskam (New York: Academic) pp 65–107

Gill W D and Kay E 1965 Efficient low pressure sputtering in a large inverted magnetron suitable for film synthesis *Rev. Sci. Instrum.* **36** 277–82

Gnaser H 2007 Energy and angular distributions of sputtered species *Sputtering by Particle Bombardment: Experiments and Computer Calculations from Threshold to MeV Energies* (*Topics in Applied Physics* vol 110) ed R Behrisch and W Eckstein (Berlin: Springer) ch 5, pp 231–328

Goebel D M and Katz I 2008 *Fundamentals of Electric Propulsion: Ion and Hall Thrusters* (Hoboken, NJ: Wiley)

Grimm W 1968 Eine neue glimmentladungslampe für die optische emissionsspektralanalyse *Spectrochim. Acta B* **23** 443–54

Grove W R 1852 On the electro-chemical polarity of gases *Phil. Mag.* 4 **4** 498–514

Gudmundsson J T, Brenning N, Lundin D and Helmersson U 2012 The high power impulse magnetron sputtering discharge *J. Vac. Sci. Technol.* A **30** 030801

Harrison W W, Yang C and Oxley E 2003 Mass spectrometry of glow discharges *Glow Discharge Plasmas in Analytical Spectroscopy* ed R K Marcus and J A C Broekaert (Chichester: Wiley) pp 71–96

Hasselkamp D 1992 Kinetic electron emission from solid surfaces under ion bombardment *Particle Induced Electron Emission II* (*Springer Tracts in Modern Physics* vol 123) ed D Hasselkamp *et al* (Berlin: Springer) pp 1–95

Helmersson U, Lattemann M, Bohlmark J, Ehiasarian A P and Gudmundsson J T 2006 Ionized physical vapor deposition (IPVD): a review of technology and applications *Thin Solid Films* **513** 1–24

Hofer W O 1991 Angular, energy, and mass distribution of sputtered particles *Sputtering by Particle Bombardment III: Characteristics of Sputtered Particles, Technical Applications* (*Topics in Applied Physics* vol 64) ed R Behrisch and K Wittmaack (Berlin: Springer) pp 15–90

Hooper E B 1969 A review of reflex and Penning discharges *Advances in Electronics and Electron Physics* vol 27 ed L Marton and C Marton (New York: Academic) pp 295–343

Howatson A M 1976 *An Introduction to Gas Discharges* 2nd edn (Oxford: Pergamon)

Ingold J H 1978 Anatomy of the discharge *Gaseous Electronics: Electrical Discharges* vol 1 ed M Hirsh and H J Oskam (New York: Academic) pp 19–64

Ingold J H 1997 Nonequilibrium positive column *Phys. Rev. E* **56** 5932–44

Kawamura E and Ingold J H 2001 Particle in cell simulations of low pressure small radius positive column discharges *J. Phys. D: Appl. Phys.* **34** 3150–62

Kay E 1962 Impact evaporation (sputtering) and thin film growth in a glow discharge *Advances of Electronics and Electron Physics* vol 17 ed L L Marton (New York: Academic) pp 245–322

Klawuhn E, D'Couto G C, Rymer K A A P, Biberger M A and Levy K B 2000 Ionized physical-vapor deposition using a hollow-cathode magnetron source for advanced metallization *J. Vac. Sci. Technol.* A **18** 1546–9

Kolobov V I 2006 Striations in rare gas plasmas *J. Phys. D: Appl. Phys.* **39** R487–506

Kolobov V I and Tsendin L D 1995 Analytic model of the hollow cathode effect *Plasma Sources Sci. Technol.* **4** 551–60

Langmuir I 1913 The effect of space charge and residual gases on thermionic currents in high vacuum *Phys. Rev.* **2** 450–86

Lieberman M A and Lichtenberg A J 2005 *Principles of Plasma Discharges and Materials Processing* 2nd edn (New York: Wiley)

Lisovskiy V A, Artushenko K P and Yegorenkov V D 2016 Child–Langmuir law applicability for a cathode sheath description of glow discharge in hydrogen *Phys. Scr.* **91** 085601

Lisovskiy V A, Derevianko V A and Yegorenkov V D 2014 The Child–Langmuir collision laws for the cathode sheath of glow discharge in nitrogen *Vacuum* **103** 49–56

Lisovskiy V A, Derevianko V A and Yegorenkov V D 2015 DC breakdown in low-pressure CF_4 *J. Phys. D: Appl. Phys.* **48** 475201

Lisovskiy V A, Koval V A, Artushenko E P and Yegorenkov V D 2012 Validating the Goldstein–Wehner law for the stratified positive column of dc discharge in an undergraduate laboratory *Eur. J. Phys.* **33** 1537–45

Lisovskiy V A, Yakovin S D and Yegorenkov V D 2000 Low-pressure gas breakdown in uniform dc electric field *J. Phys. D: Appl. Phys.* **33** 2722–30

Mavrodineanu R 1984 Hollow cathode discharges *J. Res. Natl Bur. Stand.* **89** 143–85

Miller H C 1963 Paschen curve in nitrogen *J. Appl. Phys.* **34** 3418

Möller W and Eckstein W 1984 TRIDYN—a TRIM simulation code including dynamic composition changes *Nucl. Instrum. Methods Phys. Res.* B **2** 814–8

Möller W, Eckstein W and Biersack J 1988 TRIDYN—binary collision simulation of atomic collisions and dynamic composition changes in solids *Comput. Phys. Commun.* **51** 355–68

Mott N F and Gurney R W 1948 *Electronic Processes in Ionic Crystals* 2nd edn (Oxford: Oxford University Press)

Muhl S and Pérez A 2015 The use of hollow cathodes in deposition processes: a critical review *Thin Solid Films* **579** 174–98

Nelis T and Payling R 2003 Glow discharge optical emission spectrometry *Surface Analysis Methods in Materials Science* (*Springer Series in Surface Science* vol 23) ed D J O'Connor *et al* (Berlin: Springer) pp 553–9

Oechsner H 1975 Sputtering-a review of some recent experimental and theoretical aspects *Appl. Phys.* A **8** 185–98

Oleson N L and Cooper A W 1968 Moving striations *Advances in Electronics and Electron Physics* vol 24 ed L Marton and C Marton (New York: Academic) pp 155–278

Parilis E and Kishinevskii L 1960 Kinetic secondary electron ejection from molybdenum by cesium ions *Sov. Phys.—Solid State* **3** 885

Pekarek L 1968 Ionization waves (striations) in a discharge plasma *Sov. Phys.—Usp.* **11** 188–208

Pekárek L and Krejčí V 1962 Theory of moving striations in plasma of D-C discharge: I. Basic equation and its general solution *Czech. J. Phys.* B **12** 450–60

Penning F M 1937 Ein neues manometer für niedrige gasdrucke, insbesondere zwischen 10^{-3} und 10^{-5} mm *Physica* **4** 71–5

Petrov I, Adibi F, Greene J E, Hultman L and Sundgren J-E 1993 Average energy deposited per atom: a universal parameter for describing ion-assisted film growth? *Appl. Phys. Lett.* **63** 36–8

Phelps A V 2001 Abnormal glow discharges in Ar: experiments and models *Plasma Sources Sci. Technol.* **10** 329–43

Phelps A V and Petrović Z L 1999 Cold-cathode discharges and breakdown in argon: surface and gas phase production of secondary electrons *Plasma Sources Sci. Technol.* **8** R21–44

Phelps A V, Pitchford L C, Pédoussat C and Donkó Z 1999 Use of secondary-electron yields determined from breakdown data in cathode-fall models for Ar *Plasma Sources Sci. Technol.* **8** B1–2

Pillow M E 1981 A critical review of spectral and related physical properties of the hollow cathode discharge *Spectrochim. Acta* B **36** 821–43

Pons-Corbeau J 1985 Study of emission and sputtering yields in some alloys and oxide by glow discharge optical spectrometry: quantification of analysis *Surf. Interface Anal.* **7** 169–76

Raizer Y P 1991 *Gas Discharge Physics* (Berlin: Springer)

Roth J R 1995 *Industrial Plasma Engineering: Principles* vol 1 (Bristol: Institute of Physics Publishing)

Schiller S, Goedicke K, Reschke J, Kirchhoff V, Schneider S and Milde F 1993 Pulsed magnetron sputter technology *Surf. Coat. Technol.* **61** 331–7

Schoenbach K H, Moselhy M and Shi W 2004 Self-organization in cathode boundary layer microdischarges *Plasma Sources Sci. Technol.* **13** 177–85

Schottky W 1924 Diffusiontheorie der positiven säule *Phys. Zeitscrift* **25** 635–40

Sellers J 1998 Asymmetric bipolar pulsed DC: the enabling technology for reactive PVD *Surf. Coat. Technol.* **98** 1245–50

Sigmund P 1969 Theory of sputtering: I. Sputtering yield of amorphous and polycrystalline targets *Phys. Rev.* **184** 383–416

Sivoš J, Škoro N, Marić D, Malović G and Petrović Z L 2015 Breakdown and dc discharge in low-pressure water vapour *J. Phys. D: Appl. Phys.* **48** 424011

Stuart R V, Wehner G K and Anderson G S 1969 Energy distribution of atoms sputtered from polycrystalline metals *J. Appl. Phys.* **40** 803–12

Thompson M W 1968 The energy spectrum of ejected atoms during the high energy sputtering of gold *Phil. Mag.* **18** 377–414

Thompson M W 1981 Physical mechanisms of sputtering *Phys. Rep.* **69** 335–71

Thornton J A 1978 Magnetron sputtering: basic physics and application to cylindrical magnetrons *J. Vac. Sci. Technol.* **15** 171–7

Thornton J A and Greene J E 1994 Sputter deposition processes *Handbook of Deposition Technologies for Films and Coatings: Science, Technology and Applications* ed R F Bunshah 2nd edn (Park Ridge, NJ: Noyes Publications) pp 275–345

Thornton J A and Penfold A S 1978 Cylindrical magnetron sputtering *Thin Film Processes* vol 4 ed J L Vossen and W Kern (New York: Academic) pp 75–113

Tonks L and Langmuir I 1929 A general theory of the plasma of an arc *Phys. Rev.* **34** 876–922

Tsendin L D 1995 Electron kinetics in non-uniform glow discharge plasmas *Plasma Sources Sci. Technol.* **4** 200–11

Uhrlandt D and Winkler R 1996 Radially inhomogeneous electron kinetics in the DC column plasma *J. Phys. D: Appl. Phys.* **29** 315–20

Vossen J L and Cuomo J J 1978 Glow discharge sputter deposition *Thin Film Processes* vol 4 ed J L Vossen and W Kern (New York: Academic) pp 11–73

Škoro N, Marić D, Malović G, Graham W G and Petrović Z L 2011 Electrical breakdown in water vapor *Phys. Rev.* E **84** 055401

Škoro N, Marić D and Petrović Z L 2008 Effective discharge area of nonequilibrium DC discharges *IEEE Trans. Plasma Sci.* **36** 994–5

Wagenaars E, Bowden M D and Kroesen G M W 2005 Plasma emission imaging of a low-pressure argon breakdown *Plasma Sources Sci. Technol.* **14** 342–50

Wagenaars E, Bowden M D and Kroesen G M W 2007 Measurements of electric-field strengths in ionization fronts during breakdown *Phys. Rev. Lett.* **98** 075002

Wagenaars E, Perriëns N W B, Brok W J M, Bowden M D, van Veldhuizen E M and Kroesen G M W 2006 Pre-breakdown light emission phenomena in low-pressure argon between parabolic electrodes *J. Phys. D: Appl. Phys.* **39** 3831–7

Waits R K 1978 Planar magnetron sputtering *J. Vac. Sci. Technol.* **15** 179–87

Wasa K and Hayakawa S 1969 Low pressure sputtering system of the magnetron type *Rev. Sci. Instrum.* **40** 693–7

Watanabe S and Oleson N L 1955 Traveling density waves in positive columns *Phys. Rev.* **99** 1701–4

Weber L F 1985 Plasma displays *Flat-Panel Displays and CRTs* ed L E Tannas (New York: Van Nostrand–Reinhold) pp 352–434

Westwood W D 1976 Glow discharge sputtering *Prog. Surf. Sci.* **7** 71–111

Window B and Savvides N 1986 Charged particle fluxes from planar magnetron sputtering sources *J. Vac. Sci. Technol.* A **4** 196–202

Wright A W 1877a On a new process for the electrical deposition of metals, and for constructing metal-covered glass specula *Am. J. Sci. Arts* **14** 169–78

Wright A W 1877b On the production of transparent metallic films by the electrical discharge in exhausted tubes *Am. J. Sci. Arts* **14** 49–55

Wright M and Beardow T 1986 Design advances and applications of the rotatable cylindrical magnetron *J. Vac. Sci. Technol.* A **4** 388–92

Yamamura Y and Tawara H 1996 Energy dependence of ion-induced sputtering yields from monoatomic solids at normal incidence *At. Data Nucl. Data Tables* **62** 149–253

Ziegler J F, Biersack J P and Ziegler M D 2008 *SRIM—The Stopping and Range of Ions in Matter* (Chester, MD: SRIM Co.)

Ziegler J F, Ziegler M D and Biersack J P 2010 SRIM—the stopping and range of ions in matter (2010) *Nucl. Instrum. Methods Phys. Res.* B **268** 1818–23